

AP600 DOCUMENT COVER SHEET

TDC

IDS

I

S

Form 58202G(5/94) [t:\xxxx\wpf.1x]

AP600 CENTRAL FILE USE ONLY

0058.FRM

RFS#:

RFS ITEM #:

AP600 DOCUMENT NO. MT03-S3C-025	REVISION NO. 1	Page 1 of 57	ASSIGNED TO
---	--------------------------	--------------	-------------

ALTERNATE DOCUMENT NUMBER: N/A

WORK BREAKDOWN #: ME

DESIGN AGENT ORGANIZATION: **ANSALDO**

TITLE: **HYDRODYNAMIC LOADS ON VESSEL HEAD SUPPORT COLUMN AND ADS PIPING
INDUCED BY ADS BLOWDOWN**

ATTACHMENTS:	DCP #/REV. INCORPORATED IN THIS DOCUMENT REVISION:
CALCULATION/ANALYSIS REFERENCE:	

ELECTRONIC FILENAME	ELECTRONIC FILE FORMAT	ELECTRONIC FILE DESCRIPTION
MT3S3C25.doc	Word Perfect 5.1	Document Text

(C) WESTINGHOUSE ELECTRIC CORPORATION 1997**WESTINGHOUSE PROPRIETARY CLASS 2**

This document contains information proprietary to Westinghouse Electric Corporation; it is submitted in confidence and is to be used solely for the purpose for which it is furnished and returned upon request. This document and such information is not to be reproduced, transmitted, disclosed or used otherwise in whole or in part without prior written authorization of Westinghouse Electric Corporation, Energy Systems Business Unit, subject to the legends contained hereof.

WESTINGHOUSE PROPRIETARY CLASS 2C

This document is the property of and contains Proprietary information owned by Westinghouse Electric Corporation and/or its subcontractors and suppliers. It is transmitted to you in confidence and trust, and you agree to treat this document in strict accordance with the terms and conditions of the agreement under which it was provided to you.

WESTINGHOUSE CLASS 3 (NON PROPRIETARY)

COMPLETE 1 IF WORK PERFORMED UNDER DESIGN CERTIFICATION OR COMPLETE 2 IF WORK PERFORMED UNDER FOAKE.

1 DOE DESIGN CERTIFICATION PROGRAM - GOVERNMENT LIMITED RIGHTS STATEMENT [See page 2]

Copyright statement: A license is reserved to the U.S. Government under contract DE-AC03-90SF18495.

DOE CONTRACT DELIVERABLES (DELIVERED DATA)

Subject to specified exceptions, disclosure of this data is restricted until September 30, 1995 or Design Certification under DOE contract DE-AC03-90SF18495, whichever is later.

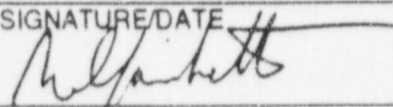
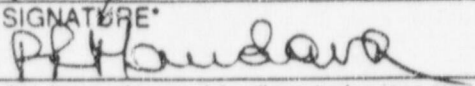
EPRI CONFIDENTIAL: NOTICE: 1 2 3 4 5 CATEGORY: A B C D E F

2 ARC FOAKE PROGRAM - ARC LIMITED RIGHTS STATEMENT [See page 2]

Copyright statement: A license is reserved to the U.S. Government under contract DE-FC02-NE34267 and subcontract ARC-93-3-SC-001.

ARC CONTRACT DELIVERABLES (CONTRACT DATA)

Subject to specified exceptions, disclosure of this data is restricted under ARC Subcontract ARC-93-3-SC-001.

ORIGINATOR	SIGNATURE/DATE	
ROBERTO GAMBETTA	 April 3, 1998	
AP600 RESPONSIBLE MANAGER	SIGNATURE*	APPROVAL DATE
		4/7/98

*Approval of the responsible manager signifies that document is complete, all required reviews are complete, electronic file is attached and document is

9804130461 980407
PDR ADDCK 05200003
A PDR

Form 58202G(5/94)

LIMITED RIGHTS STATEMENTS

DOE GOVERNMENT LIMITED RIGHTS STATEMENT

- (A) These data are submitted with limited rights under government contract No. DE-AC03-80SF18195. These data may be reproduced and used by the government with the express limitation that they will not, without written permission of the contractor, be used for purposes of manufacture nor disclosed outside the government; except that the government may disclose these data outside the government for the following purposes, if any, provided that the government makes such disclosure subject to prohibition against further use and disclosure:
- (i) This "Proprietary Data" may be disclosed for evaluation purposes under the restrictions above.
 - (ii) The "Proprietary Data" may be disclosed to the Electric Power Research Institute (EPRI), electric utility representatives and their direct consultants, excluding direct commercial competitors, and the DOE National Laboratories under the prohibitions and restrictions above.
- (B) This notice shall be marked on any reproduction of these data, in whole or in part.

ARC LIMITED RIGHTS STATEMENT:

This proprietary data, furnished under Subcontract Number ARC-93-3-SC-001 with ARC may be duplicated and used by the government and ARC, subject to the limitations of Article H-17.F. of that subcontract, with the express limitations that the proprietary data may not be disclosed outside the government or ARC, or ARC's Class 1 & 3 members or EPRI or be used for purposes of manufacture without prior permission of the Subcontractor, except that further disclosure or use may be made solely for the following purposes:

This proprietary data may be disclosed to other than commercial competitors of Subcontractor for evaluation purposes of this subcontract under the restriction that the proprietary data be retained in confidence and not be further disclosed, and subject to the terms of a non-disclosure agreement between the Subcontractor and that organization, excluding DOE and its contractors.

DEFINITIONS

CONTRACT/DELIVERED DATA — Consists of documents (e.g. specifications, drawings, reports) which are generated under the DOE or ARC contracts which contain no background proprietary data.

EPRI CONFIDENTIALITY / OBLIGATION NOTICES

NOTICE 1: The data in this document is subject to no confidentiality obligations.

NOTICE 2: The data in this document is proprietary and confidential to Westinghouse Electric Corporation and/or its Contractors. It is forwarded to recipient under an obligation of Confidence and Trust for limited purposes only. Any use, disclosure to unauthorized persons, or copying of this document or parts thereof is prohibited except as agreed to in advance by the Electric Power Research Institute (EPRI) and Westinghouse Electric Corporation. Recipient of this data has a duty to inquire of EPRI and/or Westinghouse as to the uses of the information contained herein that are permitted.

NOTICE 3: The data in this document is proprietary and confidential to Westinghouse Electric Corporation and/or its Contractors. It is forwarded to recipient under an obligation of Confidence and Trust for use only in evaluation tasks specifically authorized by the Electric Power Research Institute (EPRI). Any use, disclosure to unauthorized persons, or copying this document or parts thereof is prohibited except as agreed to in advance by EPRI and Westinghouse Electric Corporation. Recipient of this data has a duty to inquire of EPRI and/or Westinghouse as to the uses of the information contained herein that are permitted. This document and any copies or excerpts thereof that may have been generated are to be returned to Westinghouse, directly or through EPRI, when requested to do so.

NOTICE 4: The data in this document is proprietary and confidential to Westinghouse Electric Corporation and/or its Contractors. It is being revealed in confidence and trust only to Employees of EPRI and to certain contractors of EPRI for limited evaluation tasks authorized by EPRI. Any use, disclosure to unauthorized persons, or copying of this document or parts thereof is prohibited. This Document and any copies or excerpts thereof that may have been generated are to be returned to Westinghouse, directly or through EPRI, when requested to do so.

NOTICE 5: The data in this document is proprietary and confidential to Westinghouse Electric Corporation and/or its Contractors. Access to this data is given in Confidence and Trust only at Westinghouse facilities for limited evaluation tasks assigned by EPRI. Any use, disclosure to unauthorized persons, or copying of this document or parts thereof is prohibited. Neither this document nor any excerpts therefrom are to be removed from Westinghouse facilities.

EPRI CONFIDENTIALITY / OBLIGATION CATEGORIES

CATEGORY "A" — (See Delivered Data) Consists of CONTRACTOR Foreground Data that is contained in an issued reported.

CATEGORY "B" — (See Delivered Data) Consists of CONTRACTOR Foreground Data that is not contained in an issued report, except for computer programs.

CATEGORY "C" — Consists of CONTRACTOR Background Data except for computer programs.

CATEGORY "D" — Consists of computer programs developed in the course of performing the Work.

CATEGORY "E" — Consists of computer programs developed prior to the Effective Date or after the Effective Date but outside the scope of the Work.

CATEGORY "F" — Consists of administrative plans and administrative reports.

x

Table of Contents

Abbreviations

REFERENCES

1. SCOPE

2. METHODOLOGY

3. RESULTS

3.1 Support Column

3.2 Vertical ADS discharge Piping

3.3 Horizontal ADS discharge Piping

4. CONCLUSION

FIGURES

Abbreviations

AD	Acceleration Drag
ADS	Automatic Depressurization System
IRWST	In-Containment Refueling Water Storage Tank
PRHR	Passive Residual Heat Removal
PRZ	Pressurizer
PSD	Power Spectral Density
VD	Steady-Velocity Drag

REFERENCES

1. Gambetta R. - Drag Forces on a SUBMERGED STRUCTURE induced by sparger steam oscillations;
Ansaldo Doc. no. STU-0440-SRPX-0050-000, May 1994
2. Macco A. - ADS Discharge Investigation and IRWST Hydrodynamic Global Analysis;
Ansaldo Doc. no. MT03-S3C-012 , April 1996
- a1. Gambetta R.- The Phenomenon of the Pool Bubble Oscillations following a Relief Valve Air Clearing Event:
Analytical and Experimental Investigation;
Ansaldo, Doc. # STU 0440 SRPX 0025 000, march 1994
- a2. Traversone - Source Term Evaluation in Model Tank;
Ansaldo, Doc. # ADP 2110 TCLX C01 8000 febr. 1993
- a3. Dernetti P. - Analysis Plan of Ansaldo IRWST
Hydrodynamic Analysis;
Ansaldo, Doc. # ADP 2110 TCLX C01 0000 june 1991
- a4. Venturini A. - PRECCI: a Computer Code to Calculate the Normalized Pressure Distribution on Pool Boundaries due to Quencher Water and Air Clearing Loads;
Ansaldo AMN, Doc. # 400 RT 6203, sept. 1980
- c1. Otnes R. K. - Digital Time Series Analysis;
John Wiley & Sons, 1972
- c2. Milne L. M. - Theoretical Hydrodynamics;
MACMILLAN, 1968

- d1. Arinobu M. - Studies on the Dynamic Phenomena caused
by Steam Condensation in Water;
ANS/ASME/NRC Int. Meet. on Nucl.
React. Thermal-Hydraulics, Saratoga, 1980
- d2. Narai H. - Fluid and Pressure Oscillations occurring at
Aya I. Direct Contact Condensation of Steam Flow
with Cold Water;
Nucl. Engin & Design 95 (1986) 35-45
- d3. Moody F. J. - Dynamic and Thermal Behaviour of Hot
Gas Bubbles Discharged into Water;
Nucl. Engin. and Design, 95, 47-54, 1986
- d4. Paidoussis - A Semi-potential Flow Theory for the Dynamics
of Cylinder Arrays in Cross Flow;
Symp. of flow induced vibrations,
ASME winter meet., 1984
- d5. Wood B. D. - Determination of Pressure Fields in a Suppression Pool
by means of Green's Functions and Comparison
with Method of Images and a Finite Difference Solution;
Nucl. Engin. and Des., 61, 1980

1. SCOPE

This technical note presents a conservative evaluation of the dynamic loads exerted on the IRWST submerged structures support columns and ADS piping following the ADS actuation and subsequent two-phase mixture blow down.

The calculation has been performed using the simplified approach of a potential flow in an infinite (or semi-infinite) pool, which assumes an oscillating steam bubble around the sparger center or in the ADS discharge region.

The approach used in this work coincides with the methodology developed to compute the dynamics loads on the PRHR Heat Exchanger Tubes.

The general aspects of the methodology are reported in section 2 together with specific assumptions used to compute loads on head support columns and ADS piping.

Section 3 presents the final loads on both structures to be used for structural analysis evaluation.

Conclusions are outlined in section 4.

2. METHODOLOGY

The methodology used in this work is described in this section.

The methodology utilized for the evaluation of the hydrodynamics loads on the support column is applied also to evaluate the loads on the vertical ADS discharge piping.

As far as the horizontal position of the piping, at higher elevation, is concerned, a slightly different approach is used.

Following the basic assumptions used are summarized:

- The fluid motion is assumed irrotational, thus a velocity potential function describes completely the motion state.
- In the region around the sparger, the motion is assumed incompressible. Notice that the Support Columns interest only sparger B of Fig. 1.
- The steam oscillation phenomenon occurring during blow down and pool condensation is simulated by means of an ideal vibrating bubble. The radius of the bubble (called RADIUS) has been assumed equal to the sparger arm length (4.58 ft), see Fig. 1 & 2. In this model the bubble acts as an ideal time-dependent source in the potential flow field.
- The Source Strength Rate $S'(t)$ is derived from VAPORE PHASE B930 & 330 TESTS[2]. The PE16 wall-pressure time-history of tests B930 & 330 have been selected as the most representative of the condensation-induced pressure field in the tank. A Method of Images computer program (code PRECCI, Ref. A4) has been employed to compute the function $S'(t)$ on the basis of wall pressure measurements and taking into account the VAPORE tank cylindrical geometry.
- A numerical integration allows to obtain the Source Strength time-history $S(t)$.

The Hydrodynamic Model

In order to calculate the forces exerted on submerged structures caused by condensation oscillations at the exit of the spargers during the blow down phase of an ADS actuation, a hydrodynamic model using a potential flow approach and the image technique is employed.

The effect of VAPORE tank boundaries is simulated by an array of virtual images of the real source, which is the condensation event near the sparger.

The source strength and characteristics are obtained from the VAPORE test data.

The Condensation Phenomenon

It is known that steam injection into subcooled water produces unsteady phenomena called chugging or condensation oscillation. These phenomena have been studied with a special concern to the transient phenomena in the light water reactor pressure suppression system (Ref. d1, d2).

It is known about downward venting systems that if the steam velocity is rather high, steam always condenses outside the vent pipe, and periodic pressure oscillations are observed in the pool. The steam-water interface also oscillates. These phenomena are called condensation oscillations.

A general theory of the oscillation frequency and pressure amplitude produced by condensation oscillations can be derived from linear analysis of steam bubble motion at vent tube exit. Steam bubble in the analyses (Ref. d2) has in general been assumed either of cylindrical, spherical, or hemispherical shape.

It has pointed out (Ref. d1) that if steam is injected from many small pipes or many small holes (like a sparger), the pool walls will experience much smaller pressure amplitudes. The smaller diameters of the pipes and holes will produce the smaller bubbles, which oscillate out of phase, thus inducing smaller pressure field amplitudes in the pool water and on the walls.

However the analytical model of the condensation phenomena at the exit of the sparger holes is not simple at all.

Sparger Condensation

The submerged steam discharge rate from orifices like those in the ADS sparger at low discharge rates may be slow enough to form single bubbles which grow and detach periodically (Ref. d3).

Higher discharge rates form gas jets, which break up into small bubbles. Around the discharge device a bubble population develops which gets a statistical equilibrium characterized by a dominant frequency and amplitude of vapor bubbles growing and collapsing. The bubbles may also coalesce to form a large region of steam separated from the subcooled water by an extended interface, which vibrates rapidly.

Since the simulation of such phenomenology requires extended experimental data and theoretical models not available at present time, the condensation oscillation event is simulated by a simplified model as follows.

The effect of the oscillatory condensation phenomenology is modeled assuming an ideal full volume of steam, hereinafter named steam bubble, which, because of the condensation occurring at the interface with cold water and mechanical interaction with pool water, periodically expands and contract through small volume oscillations. This vibration produces periodic expulsion and aspiration of liquid from the volume occupied by the steam bubble.

The volume V of the steam bubble is assumed a function of the sparger arm radius (R_s) (Ref. 1).

The concept of the single steam bubble leads to a pulsating volume which induces a time-dependent flow in the pool water.

The strength of this fluid source can be measured, in the context of the incompressible irrotational fluid theory, on the basis of the VAPORE pressure traces on the wall.

IRWST Pool Flow Field

The oscillatory condensation phenomenon at the exit of each sparger causes time-varying water flow in the IRWST pool. To describe this transient flow, effect of compressibility within the pool water is assumed to be negligible.

Fig. 1 shows the plan view of IRWST with sparger locations. In the figure letters A and B are used to identify spargers.

For an harmonic acoustical signal in water, the characteristic wave length λ , is equal to

$$\lambda = c / f \quad \text{where } c \text{ is the sound speed and } f \text{ is the excitation frequency.}$$

In the VAPORE test the highest substantial excitation frequencies are in the range of 50 to 70 Hz. For a sound speed of ~ 5000 ft/sec in water, this leads to a minimum characteristic wave length λ equal to ~ 70 ft. This value is about the radius of the IRWST (65 ft) and therefore the incompressible approach cannot be utilized in order to compute the global fluid field into the pool. For this reason the structural analysis of the pool walls requires the use of an acoustical model of the water (D'Alembert boundary-value problem) as presented in Ref. a3.

However if we limit the field of observation to the region around the discharge device incompressibility assumptions can be made.

Region close to Discharge Device

Hereinafter we refer only to the discharge of one sparger since structures object of the loads calculation (ADS discharge piping and Vessel Head Support Columns) are so close to one sparger that forces induced on such structures from the other discharge device can be considered negligible.

In the region near the steam bubble around the sparger the following condition is satisfied:

$$\lambda \gg R_s$$

Therefore near the bubble the water motion can be considered as incompressible. We make the following further assumptions:

- Friction effects can be neglected in comparison to the effects of inertia forces.
- Vorticity effects are not considered.
- The pool is infinite. Correction to account for the presence of boundaries will be considered later.

In such a manner the condensation oscillation at discharge device is simulated by a classical hydrodynamic source (Ref. c2).

We indicate with S the strength of the source, defined by

$$S = V' / 4\pi$$

where the apex indicate time derivative.

Then the velocity potential close to the sparger is written as (Ref. 1):

$$\Phi = S / r$$

An improvement of this flow field model can be carried out in order to account for the wall effect by using the image technique (Ref. 1). Since the motion respects the incompressibility requirements only in the region close to the sparger, the image technique allows us to simulate walls only near the discharge device, and not throughout all the pool.

VAPORE Tank Flow Field

Incompressibility Assumption

The dimensions of the tank are smaller than the IRWST dimensions. Therefore the incompressible approach can be applied to the flow field of the tank. This fact allows us to compute the source strength knowing the pressure traces at the wall by means of the image technique, as will be explained in the following.

Incompressibility condition :

$$\lambda \gg R_{ta}$$

where R_{ta} is the tank radius.

Since $R_{ta} \sim 12.5$ ft, the condition is satisfied.

Calculation of the Source Strength

The excitation source due to steam condensation is modeled in the same way as in the IRWST, by utilizing the concept of hydrodynamic source. The motion in the water tank is assumed everywhere incompressible, potential and non-viscous. Therefore the governing equations are represented by Laplace equation and unsteady-Bernoulli equation (Ref. c2).

It is possible to solve Laplace equation for the tank by means of the image technique, as fully explained in Ref. 1. The effect of tank boundaries is simulated by creating an array of virtual image sources and the effect of free surface is simulated by creating an array of virtual sinks.

Following Ref. 1, for a cylindrical tank with a free surface,

$$\Phi' = S' / r_{\text{eff}}$$

The geometrical factor $(1/r_{\text{eff}})$ can be computed by the Ansaldo code PRECCI (Ref. a4). The code utilizes an array of 8 diamonds centered on the hydrodynamic source as reported in Fig. 33. To introduce three dimensional modeling, two more arrays are added as reported in Fig. 34. The total number of image employed is 580.

A comparison of the method of images solution with the analytical solution given by the Green's function approach is presented in Ref. d5. The results indicate that the two methods compare favorably.

Applying unsteady-Bernoulli equation, S' can be determined after the geometric factor $(1/r_{\text{eff}})$ is known, by means of the following equation:

$$S' = (p_{\text{wall}} / \rho) * r_{\text{eff}}$$

Drag Forces on Submerged Structures in Unsteady Flow

Steam condensation vibration induces a flow field in the IRWST. The liquid motion will impose forces on submerged structures.

Since we have assumed that water motion across tubes is incompressible and irrotational, we can utilize the model and methodology developed in the frame of the air clearing phenomenology (Ref. 1) to compute the hydrodynamic forces on the tubes.

The most common force, hereafter called steady or velocity drag (VD), is a summation of skin friction and the pressure drag caused by wake formation behind structures in a moving fluid. Steady drag is predicted with the help of experimentally determined drag coefficients, based on steady flow field with negligible free stream pressure gradients.

In addition to VD, another force can exist which is caused by acceleration of the flow field about a submerged structure. Fluid acceleration is associated with a pressure gradient in the free stream, which imposes a force called acceleration drag (AD).

Structures in unsteady flows experience a combination of both steady and accelerating drag forces, which should be estimated in order to determine mechanical design requirements (Ref. 1).

Notice that in unsteady flow (with a zero mean time value) the VD contribution to the global drag force is very low and its contribution is usually neglected.

Acceleration Field

The idealized basis of this approach is that submerged structures to be considered are submerged in an infinite, spatial uniform flow with time-dependent velocity

$$v_{inf}(t)$$

and acceleration

$$\frac{d}{dt} [v_{inf}(t)]$$

The acceleration field $\frac{d}{dt} [v_{inf}(t)]$ can be calculated at each time instant.

The submerged structure is supposed to be normal to the uniform flow field (Fig. 35).

The Acceleration Drag in the Potential Flow

It is shown (Ref. a1) that the acceleration drag force (AD) has the following expression:

$$F_{ad} = \rho V_{ad} \frac{d}{dt} (v_{inf})$$

where the acceleration drag volume is defined by

$$V_{ad} = V_s + M_a / \rho$$

where M_a is the added submerged structure mass, also called hydrodynamic mass, and V_s is the volume of the submerged structure (Ref. c3).

Steady Drag Formula

Based on uniform, non-accelerating flow at velocity v_{inf} , the steady drag is expressed as follows:

$$F_{sd} = C_d \cdot A_x \cdot 1/2 \cdot \rho \cdot v_{inf}^2$$

Structures are considered submerged in a uniform flow whose direction is aligned with the x-axis, as shown in Fig. 35. The area A_x is the projection of surface body area A on a plane normal to the x-axis. C_d is a coefficient depending on the form of the body and the Reynolds number, and it is usually determined through experimental charts (see Ref. a1).

LOADS CALCULATION

Following the methodology just described the $S'(t)$ function has been determined using data from VAPOR PHASE B tests 330 & 930 using the PE16 wall pressure time histories. Starting from this source strength function $S'(t)$ the following steps have been performed.

- An $S(t)$ function has been determined through numerical integration.
- The velocity field at the bubble surface can be computed by:

$$VEL_SURF = S(t) / RADIUS^2$$

- The acceleration field at the bubble surface is computed by:

$$ACC_SURF = S'(t) / RADIUS^2$$

- The Support Column has been subdivided into 9 segments each one 3.12 ft long, in accordance to structural analysis (ANSYS code) indications.
- The velocity field at each Support Column element surface is computed by:

$$VEL_COL = S(t) / DIST^2$$

being DIST the distance from the bubble center (sparger center) to the submerged structure element (see Fig. 2).

- The acceleration field at the Support Column element surface is computed by:

$$ACC_COL = S'(t) / DIST^2$$

- The VD magnitude at the bubble surface is computed by:

$$VD(t) = VCOEF * VEL_SURF * ABS(VEL_SURF)$$

where VCOEF is $\frac{1}{2} \rho C_d A_x$ where:

A_x is the cross flow section of the structure

ρ is the water density

C_d is the Drag coefficient (chosen conservatively equal to 2.0)

- The VD magnitude at the Support Column element surface is computed by:

$$VD(t) = VCOEF * VEL_COL * ABS(VEL_COL)$$

- The AD magnitude close to the bubble surface is computed by:

$$AD(t) = ACC_SURF * ACOEF$$

where ACOEF is defined below:

$$ACOEF = RHO * \pi * DIAM^2 / 2 * HEIGHT$$

RHO = water density, = 62.9 lbm/ft³

DIAM = Support Column cross section diameter,
(= 18 inch)

HEIGHT = 3.12 FT, = Support Column element length

- The AD magnitude at the Support Column element is computed by:

$$AD(t) = ACC_COL * ACOEF$$

where ACOEF is defined as above.

- The AD & VD time-histories are algebraically added at each instant to obtain the Total Drag Force.
- Finally, forces obtained have been projected along the direction perpendicular to the Support Column axis (see Fig. 2).

- This approach presents some conservatism since:

The random character of the steam oscillations is modeled using a uniform bubble pulsating motion, where all the pool liquid moves in phase with the vibrating source.

Any dissipative or vorticity effect is neglected.

The submerged structure is assumed to be rigid, thus neglecting surface pressure reduction due to fluid-structure interaction.

It is remarkable that either the effect of the second sparger bubble or the effect of the walls are negligible since the Support Columns are very close to sparger B, and the source flow field goes down following the inverse of the squared-distance.

- Notice that the incompressible-irrotational flow assumption allows for the space-time separation of the space-time dependent pool flow field. Therefore the time-dependence of all meaningful fluid dynamics variables coincides with the time-dependence of the PE16 pressure forcing function. As a consequence, the spectral content of velocity, acceleration and drag force time-histories is identical to the PE16 spectrum throughout the whole discharge region.

ADS PIPING FORCING FUNCTIONS• Vertical Piping.

The same procedure outlined with reference to Support Column has been used for the node B, C, D of Fig. 3 (up to the curving bend) of both the discharge lines.

Note that in this case the oscillating bubble has been located at a distance equal to the sparger radius (= bubble radius) along a direction perpendicular to the vertical axis of the pipe (see Fig. 4) and rotated of 45 deg. with respect to the quencher arm (the choice of the arm is not influent). Moreover, the long segment A-----B has been subdivided into 5 element in order to make a more detailed evaluation of the forces. These elements have been indicated as B1, 2, 3, 4, 5.

On the basis of this new location of the bubble Velocity And Acceleration Drag Forces have been computed.

• Horizontal Piping.

We refer here to the piping between nodes E & I in Fig. 3. This piping is horizontal and near to the free surface. Since the discharge IRWST region is approximately a closed box, the streamlines characterizing the bubble oscillation flow pattern are deviated by the pool floor and canalized by the vertical walls towards the free surface, as depicted in Fig. 5.

Thus the horizontal piping is subjected to an oscillating flow which is practically perpendicular to its axis. To obtain a conservative evaluation of the loads on the horizontal piping the following approach has been used:

The sparger bubble has been assumed to move randomly around the quencher, positioning below any horizontal pipe element. As a consequence the condensation bubble is located under the vertical line which passes through the pipe element (1 ft long), and at the quencher elevation.

To account for the free surface effect (see Fig. 7), a bubble sink image is located above the free surface in accordance to the Method of Images. Fig. 6 shows the bubble position with respect to the piping in this approach.

Notice that the load exerted by the bubble flow on each 1ft pipe element has been assumed to act along the perpendicular from the bubble center to the pipe element axis (line OP of Fig. 6).

Notice that in the calculation of the forces acting on the HORIZONTAL PIPING, because of the different methodology utilized, the loads are given in LBF/FT.

3. RESULTS

The analysis have been performed for both tests B930 and B330 using the whole time histories. In the following figures only the B930 test (15-30 s) interval is here presented, since it presents the highest oscillation peaks.

The ADS-VAPORE pressure time-history is reported in Figs. 8 and 9.

The Source Strength Rate time-history evaluated as described in section 2 is reported in Fig. 10, whereas the Source Strength time-history is presented in Fig. 11.

The surface bubble velocity and acceleration are reported in Figs. 12 and 13 respectively. It is seen that the velocity values are very small, therefore the velocity drag is negligible and only the acceleration drag gives contribution to the calculation of the loads.

However the total drag force calculation takes into account also the VD contribution, although very small.

3.1 Support Column

Figs. 14 and 15 show the AD & VD at Support Column element no. 5 respectively. It can be observed that the velocity drag is quite negligible in comparison with acceleration drag.

Figs. from 16 to 24 report the total force time-history on the Support Column element no. 1, 2, 3, 4, 5, 6, 7, 8 and 9 respectively.

3.2 Vertical ADS discharge Piping

Figs. from 25 to 29 report the total force time-history on the segment from node A to node B, that is with reference to elements no. 1, 2, 3, 4, 5 respectively (each one 3.5 ft height, for a total height of 17.5 ft). Note that the forces are identical for both the discharge lines.

Fig. 30 shows the load time-history on segment from node B to node C, whereas Fig. 31 shows the load time-history on segment from node C to node D and higher elevations until the connection to horizontal piping.

The peak values reported are as follows: Segment 1A-1B (5 elements from bottom to top) - Elem. 1 - 200 lbf, Elem. 2 - 400 lbf, Elem. 3 - 1000 lbf, Elem. 4 - 3000 lbf, Elem. 5 - 7500 lbf. Segment 1B-1C 4000 lbf, Segment 1C-1D (bend included) 800 lbf.

3.3 Horizontal ADS discharge Piping

Fig. 32 shows the time-history on the horizontal piping from node E to node I, in LBF/FT. Notice that the forces are identical for both lines. The load peak is approximately 650 lbf/ft.

4. CONCLUSION

A Simplified Approach has been used to evaluate the Drag Forces on IRWST Support Column and ADS PIPING during the ADS blow down.

On the basis of VAPORE blow down tests, pressure forcing function time-history of Phase-B Tests 930 & 330 have been selected.

The condensation phenomenon has been simulated by means of an oscillating bubble in an infinite or semi-infinite perfect fluid pool.

On the basis of a series of described assumptions concerning the position of the condensation bubble with respect to the submerged structure of interest, the velocity and acceleration drags have been computed.

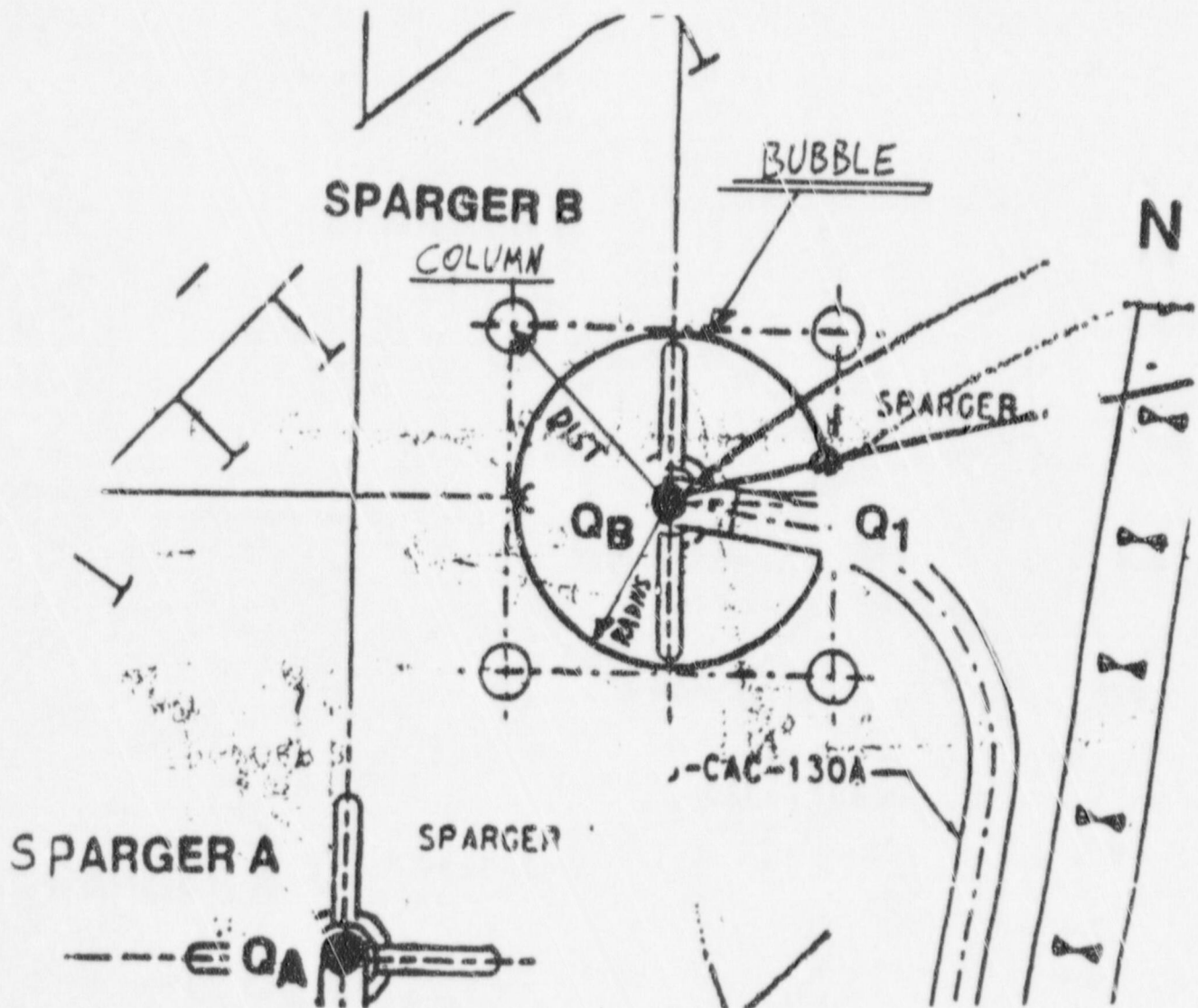
Only the ACCELERATION DRAG is significant because of the relatively high frequency content of the sparger forcing function.

The loads are vibratory with the frequency content of the experimental measurements. The load magnitude depend on the distance between the condensation bubble and the submerged structure of concern.

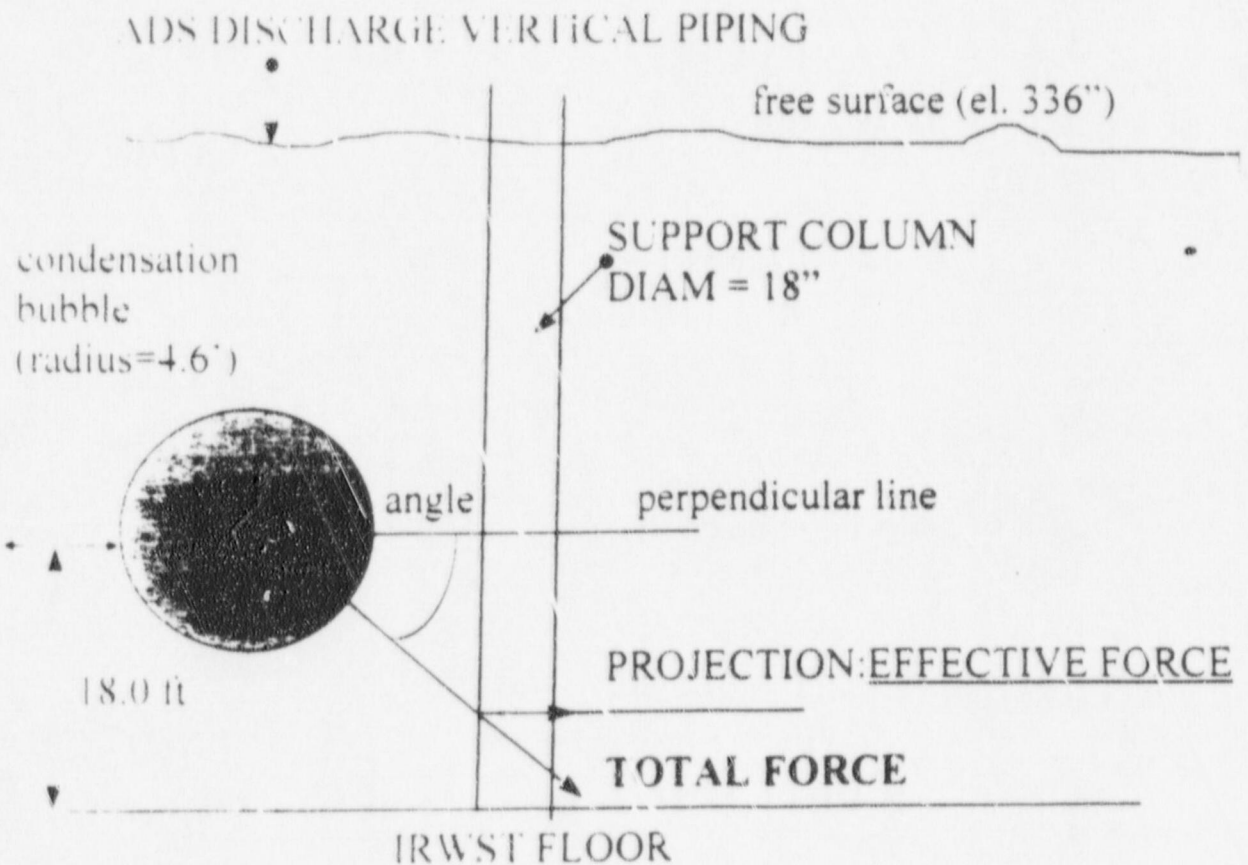
Time histories of the loads for the vessel head support column as well as for ADS discharge piping have been computed and presented.

FIGURES

1. IRWST SPARGER LOCATIONS AND IDEAL SPARGER BUBBLE



2. SUPPORT COLUMN - SPARGER BUBBLE CONFIGURATION



3. PIPING GEOMETRY AND NODING



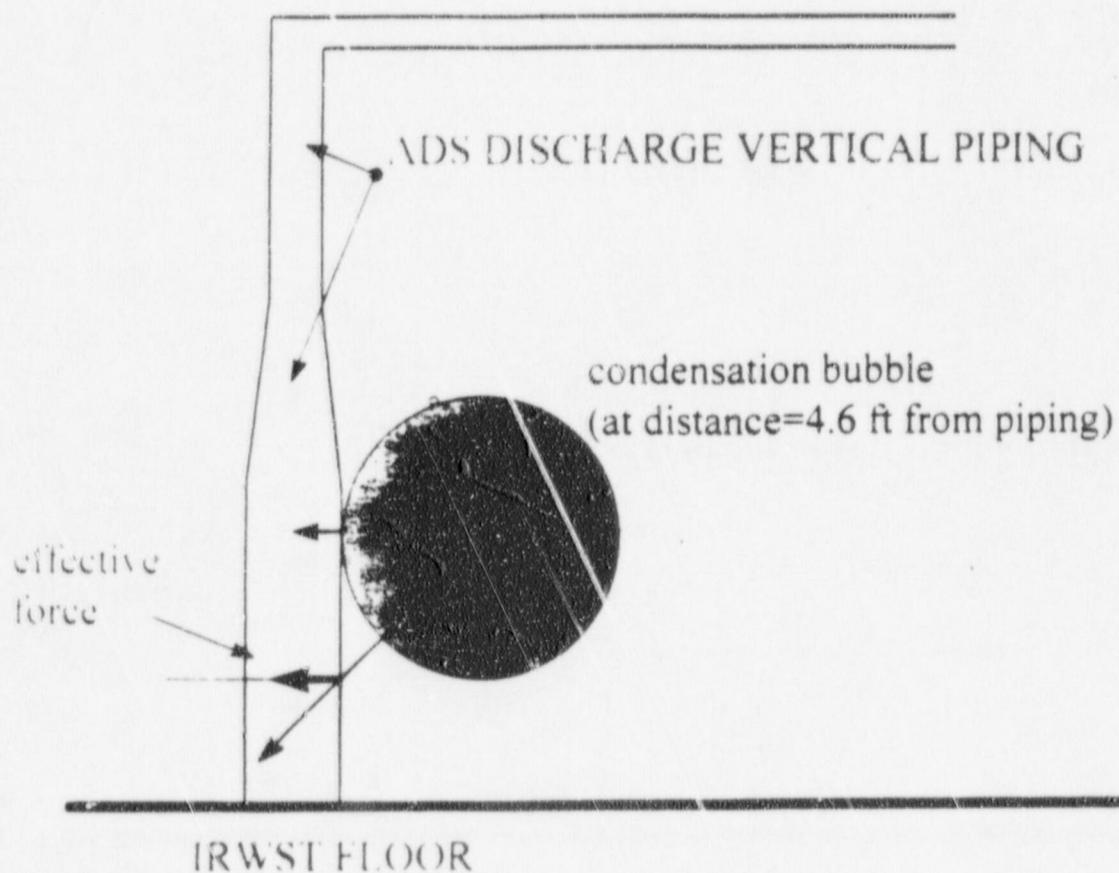
LINE NO

PXS-PL-L8308

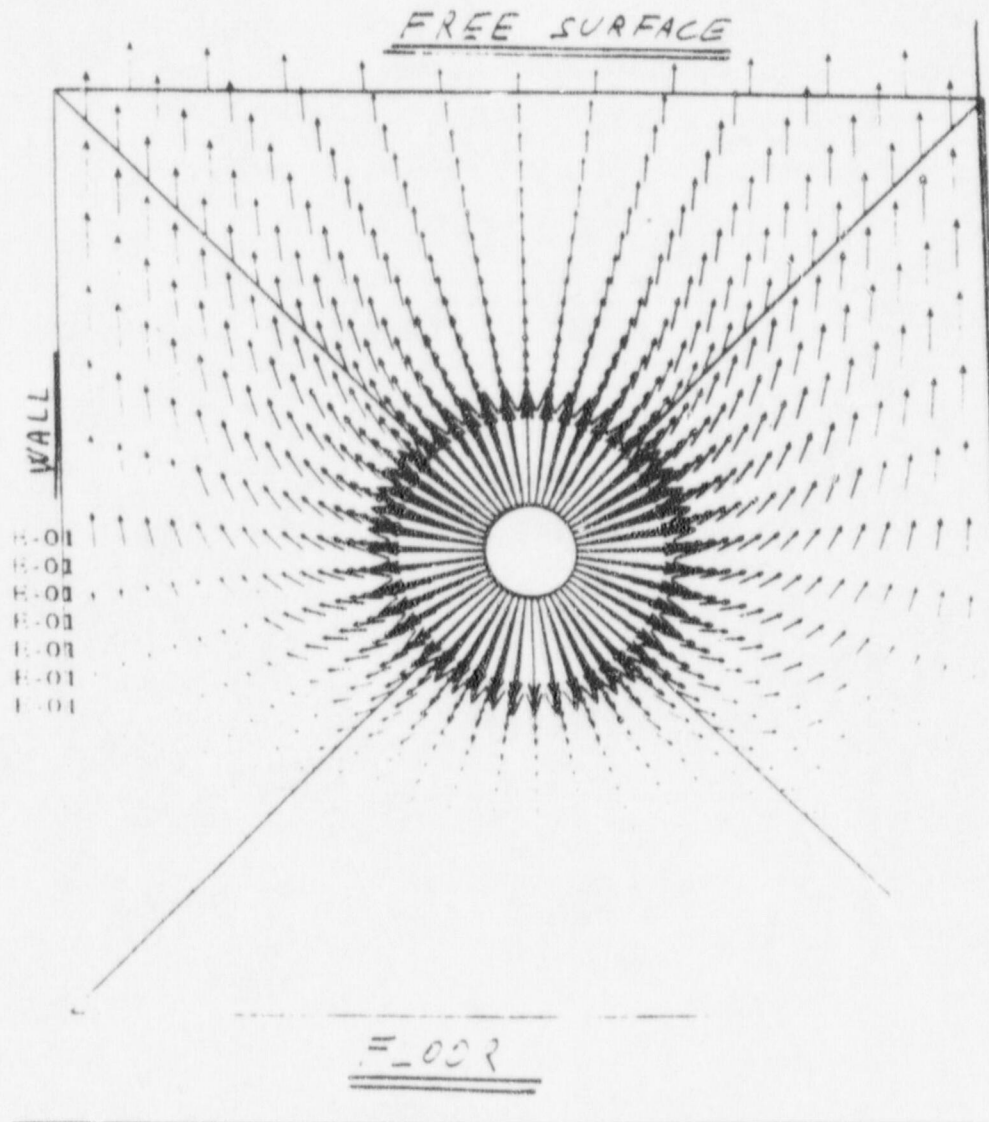
RCS-PL-L8648

MFC-PL-L7400

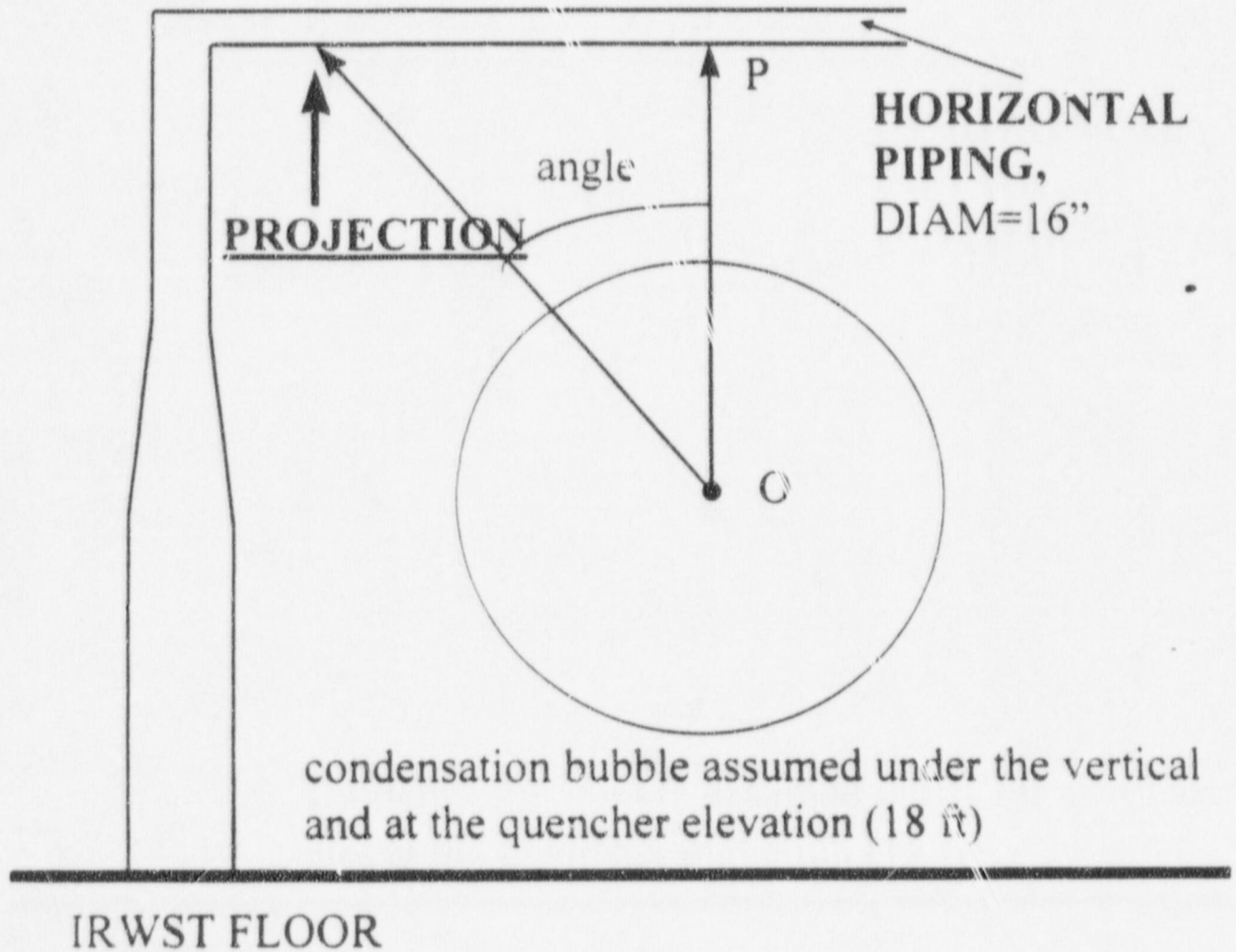
4. ADS PIPING - CONDENSATION BUBBLE CONFIGURATION



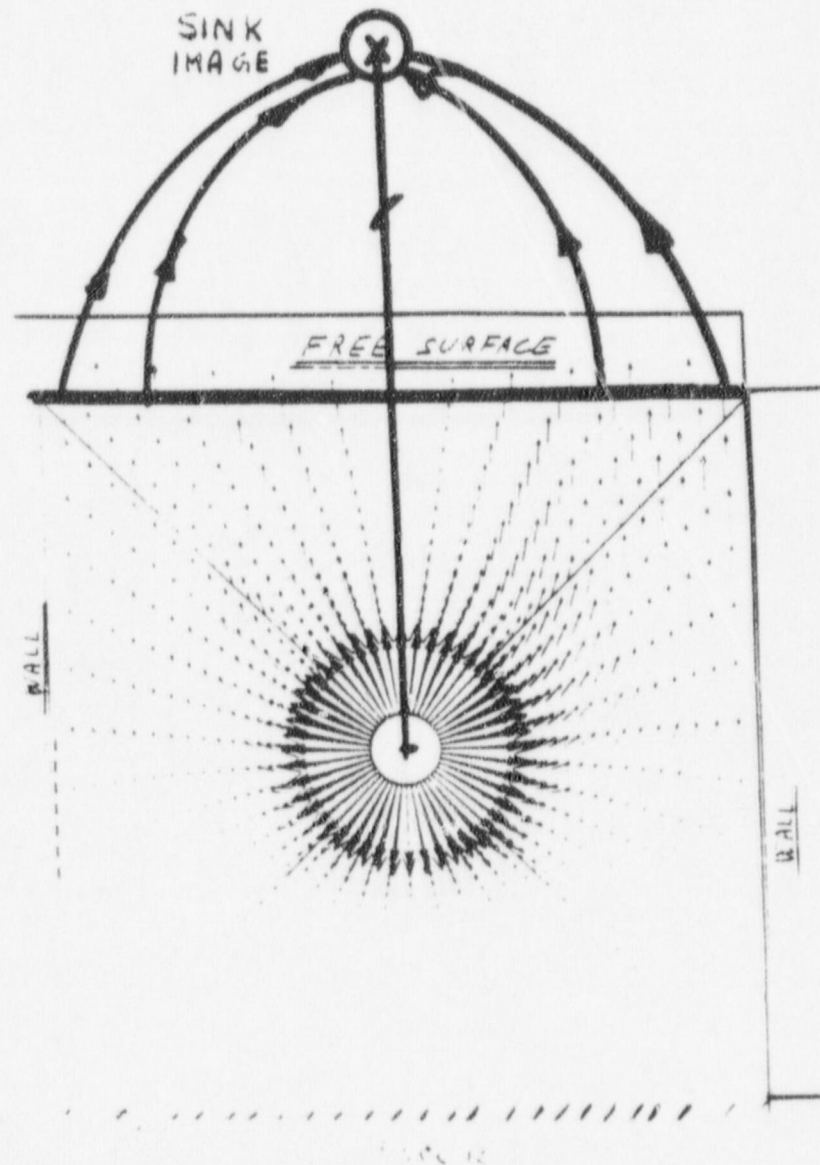
5. CLOSED BOX FLOW PATTERN



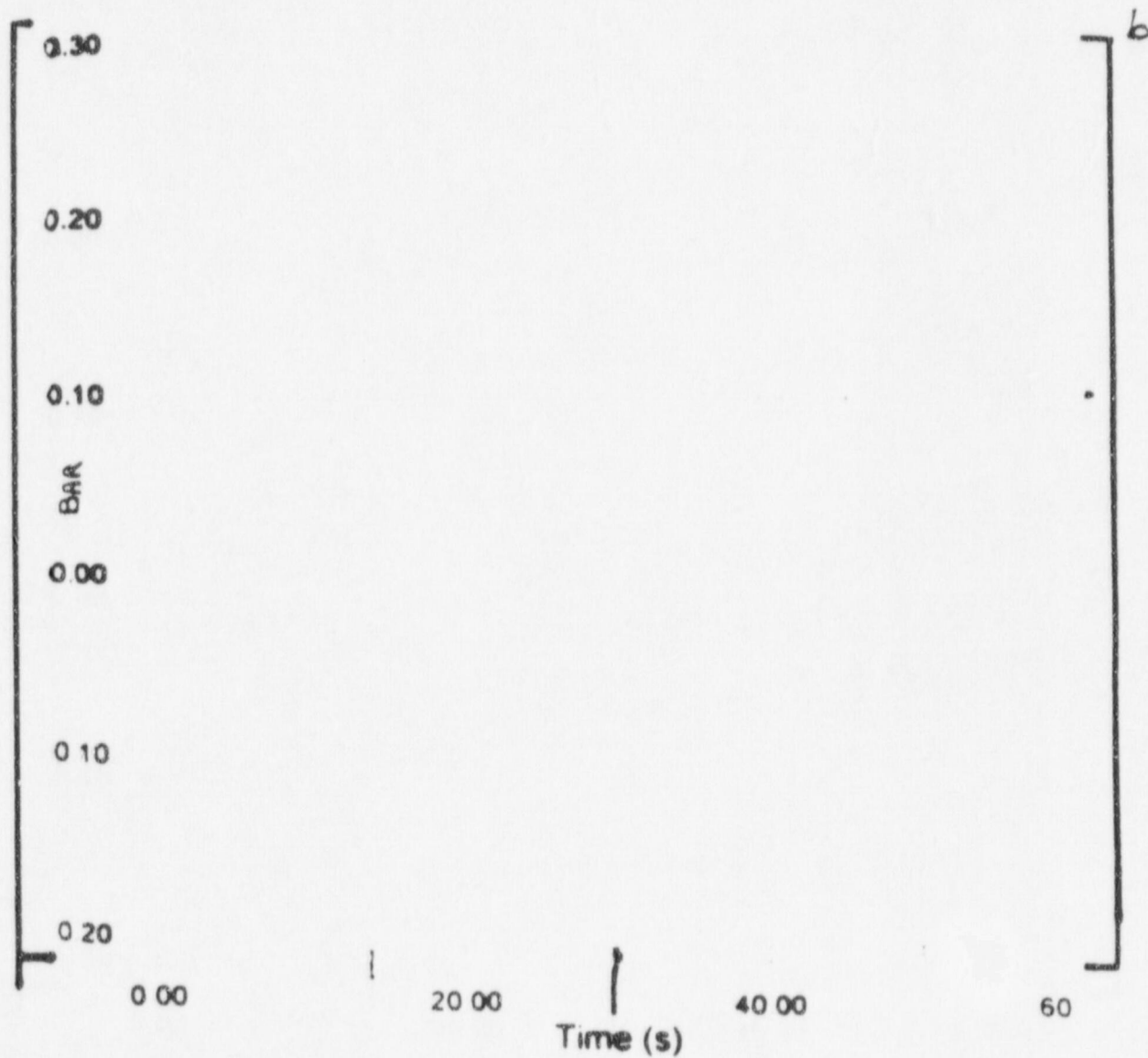
6. HORIZONTAL PIPING: APPROACH CONFIGURATION



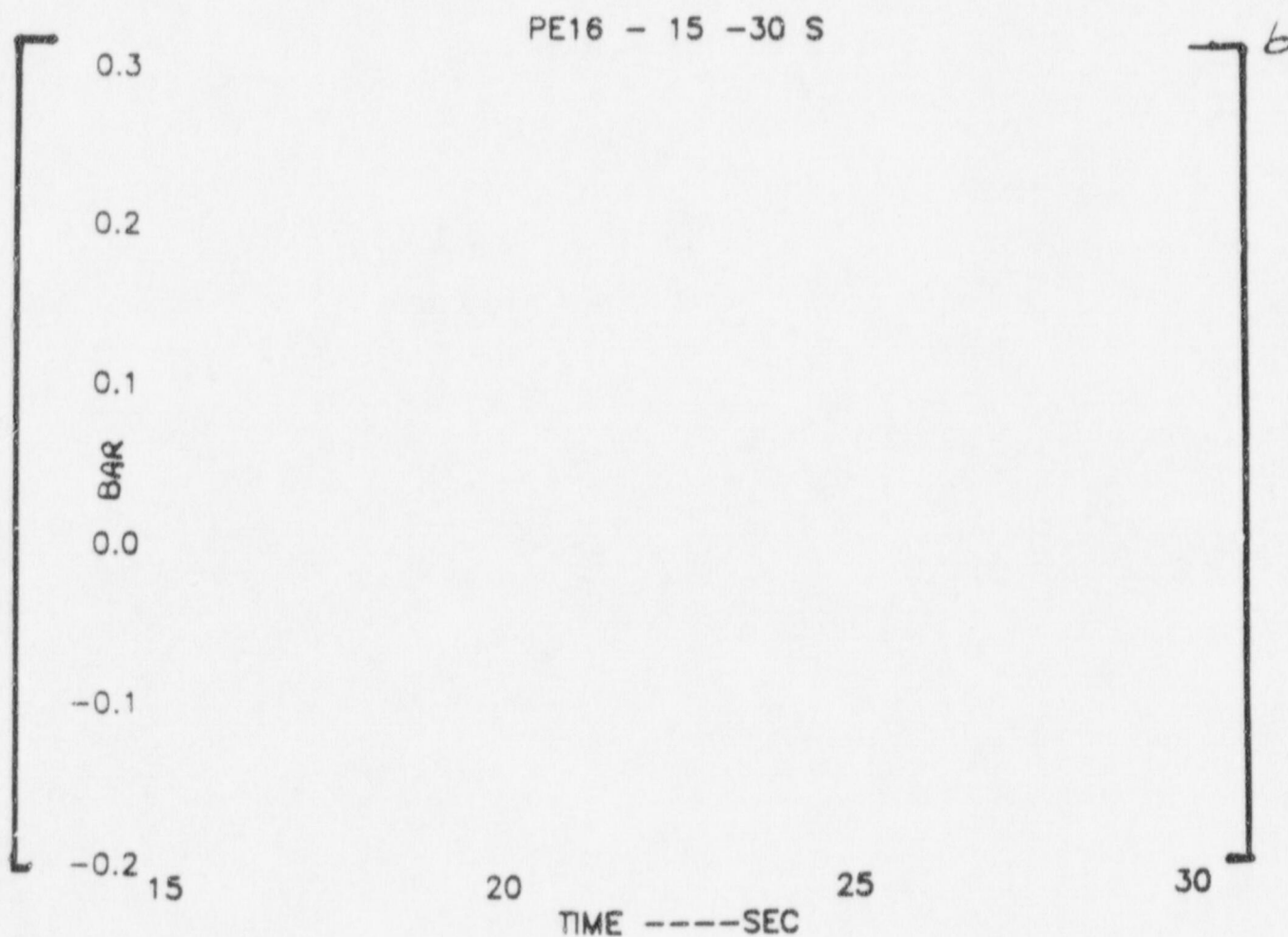
7. FREE SURFACE EFFECT AND SINK IMAGE



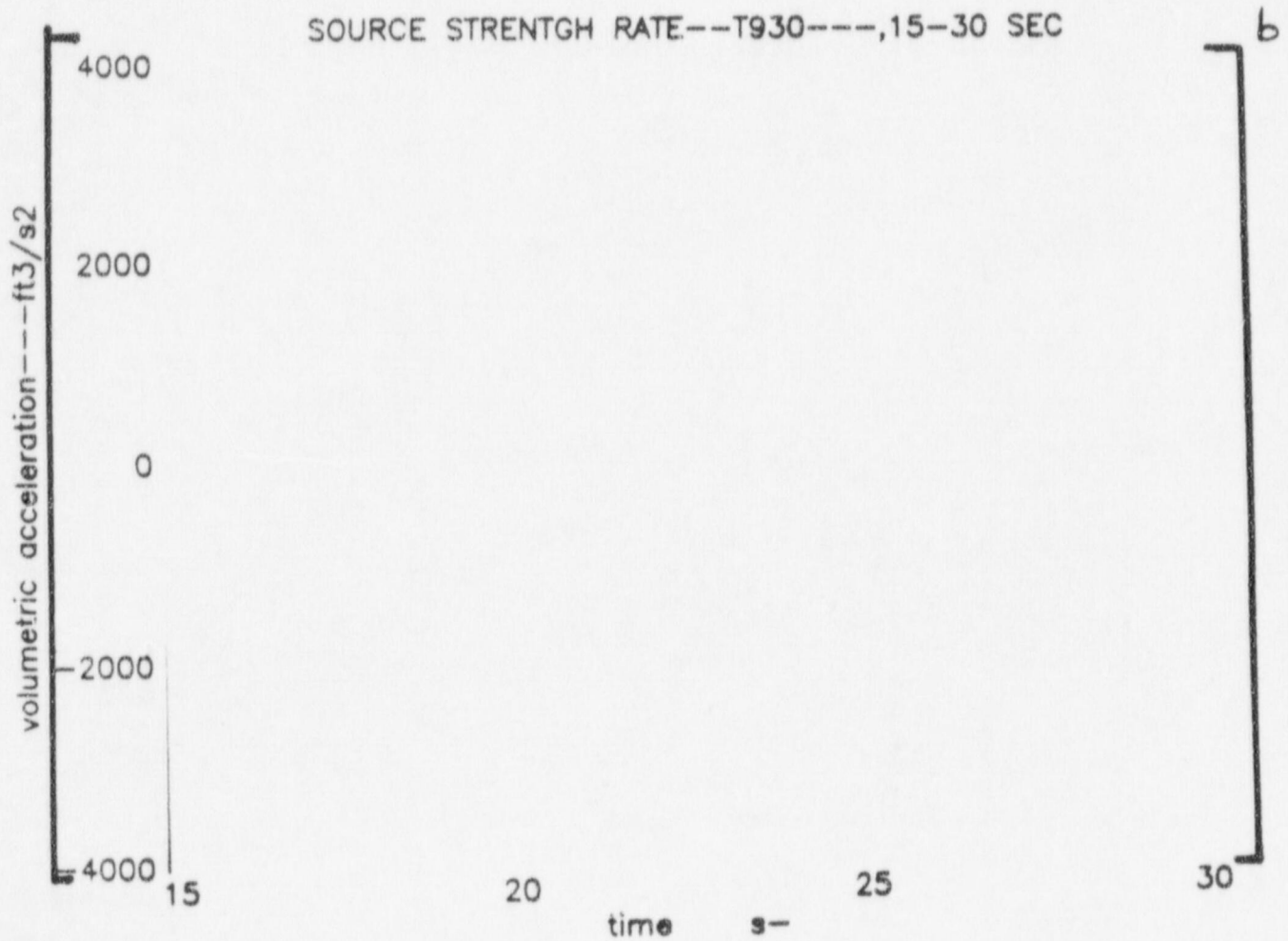
8. PHASE-B1-TEST930-PE16-PRESSURE TIME-HISTORY

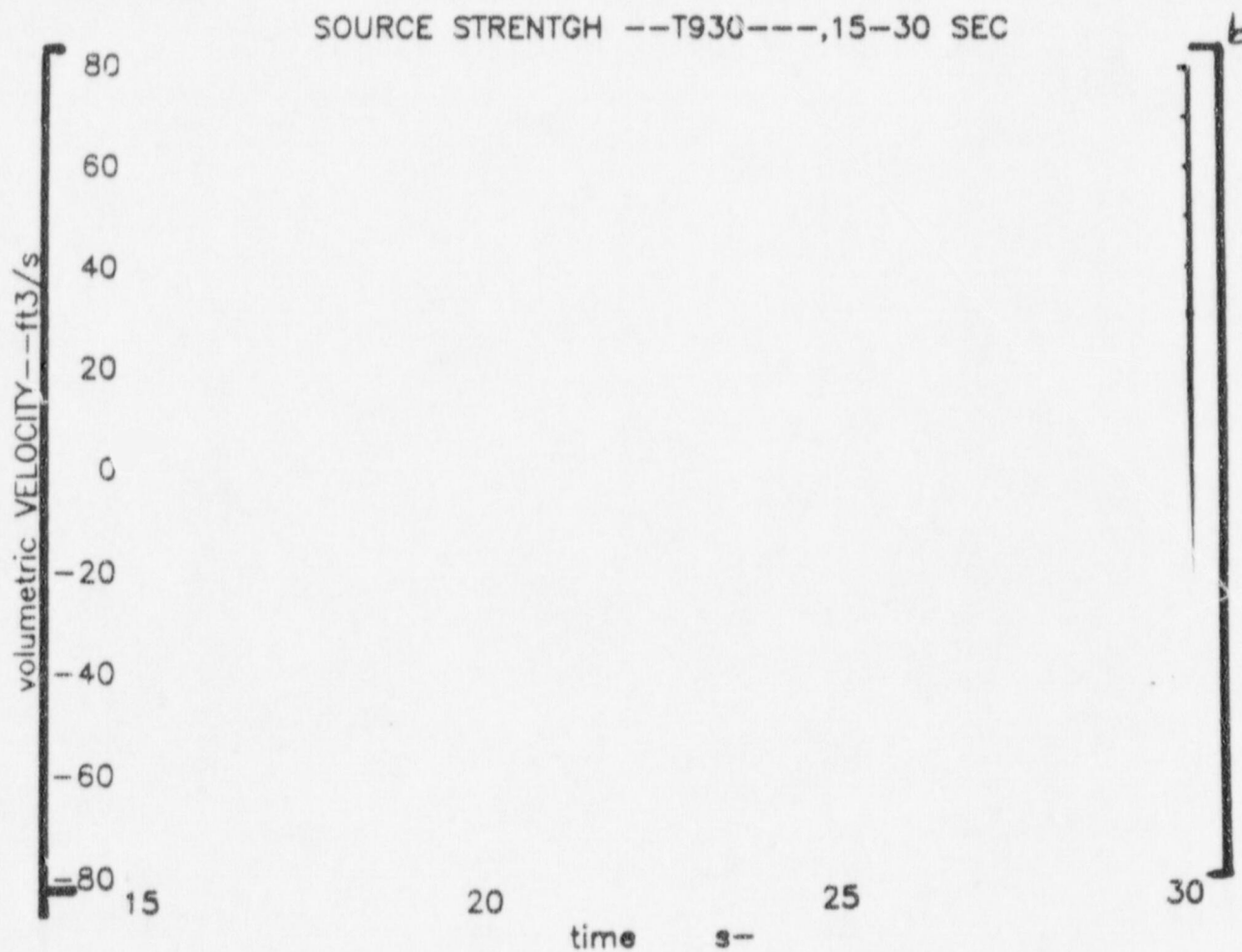


9. PHASE-B1-TEST930-PE16-PRESSURE TIME-HISTORY
(15-30 S INTERVAL)

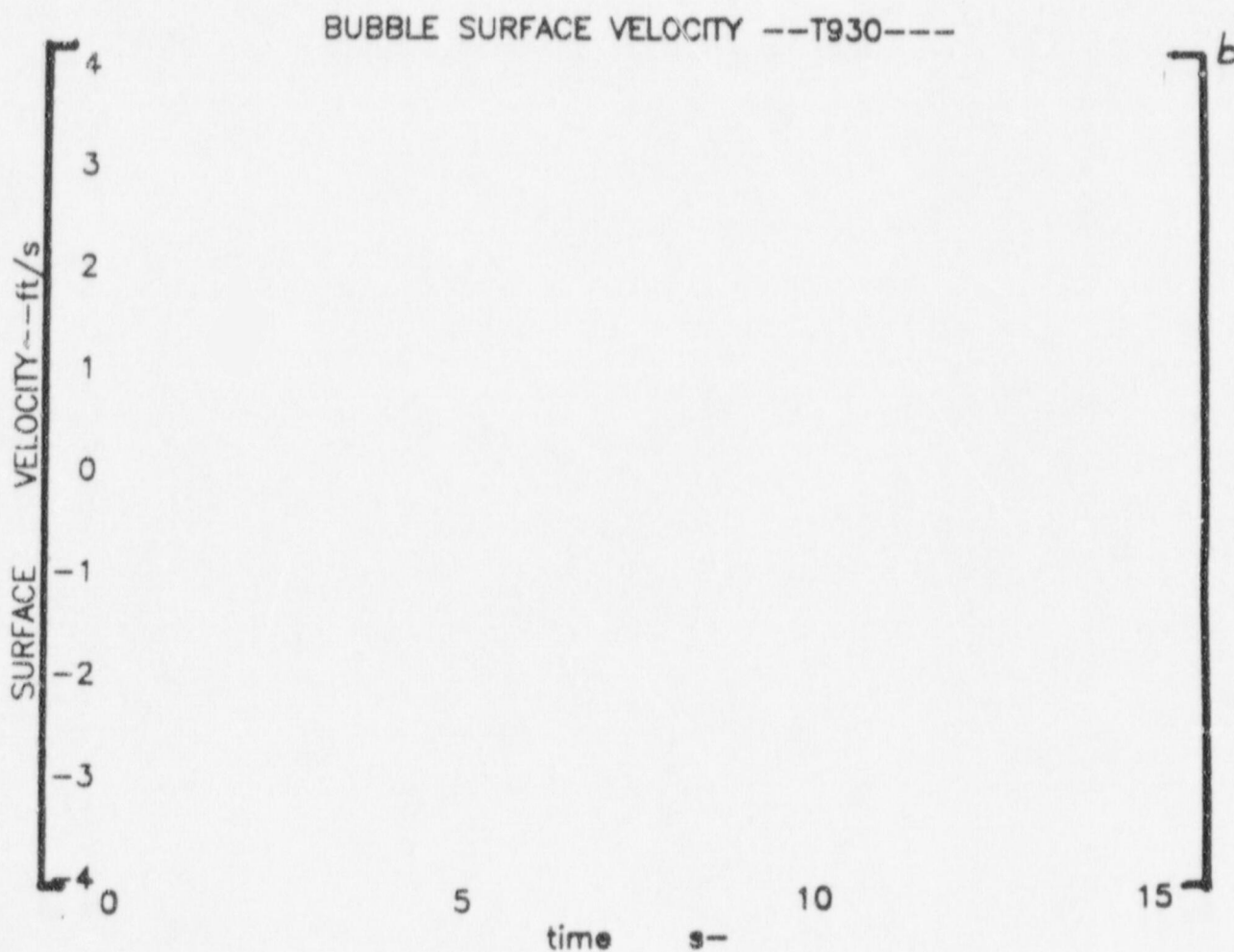


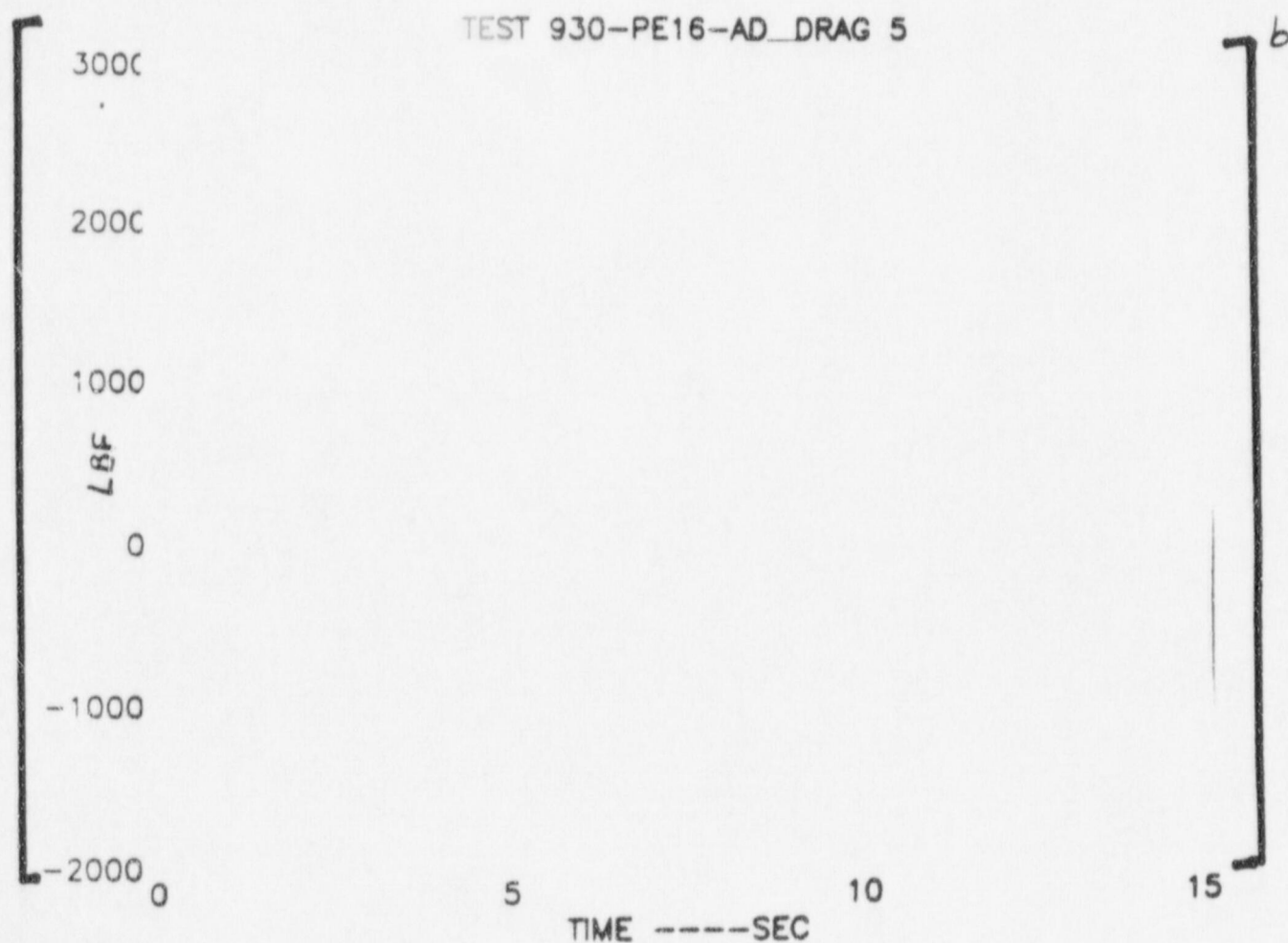
10. SOURCE STRENGTH RATE TIME-HISTORYFT3/S2

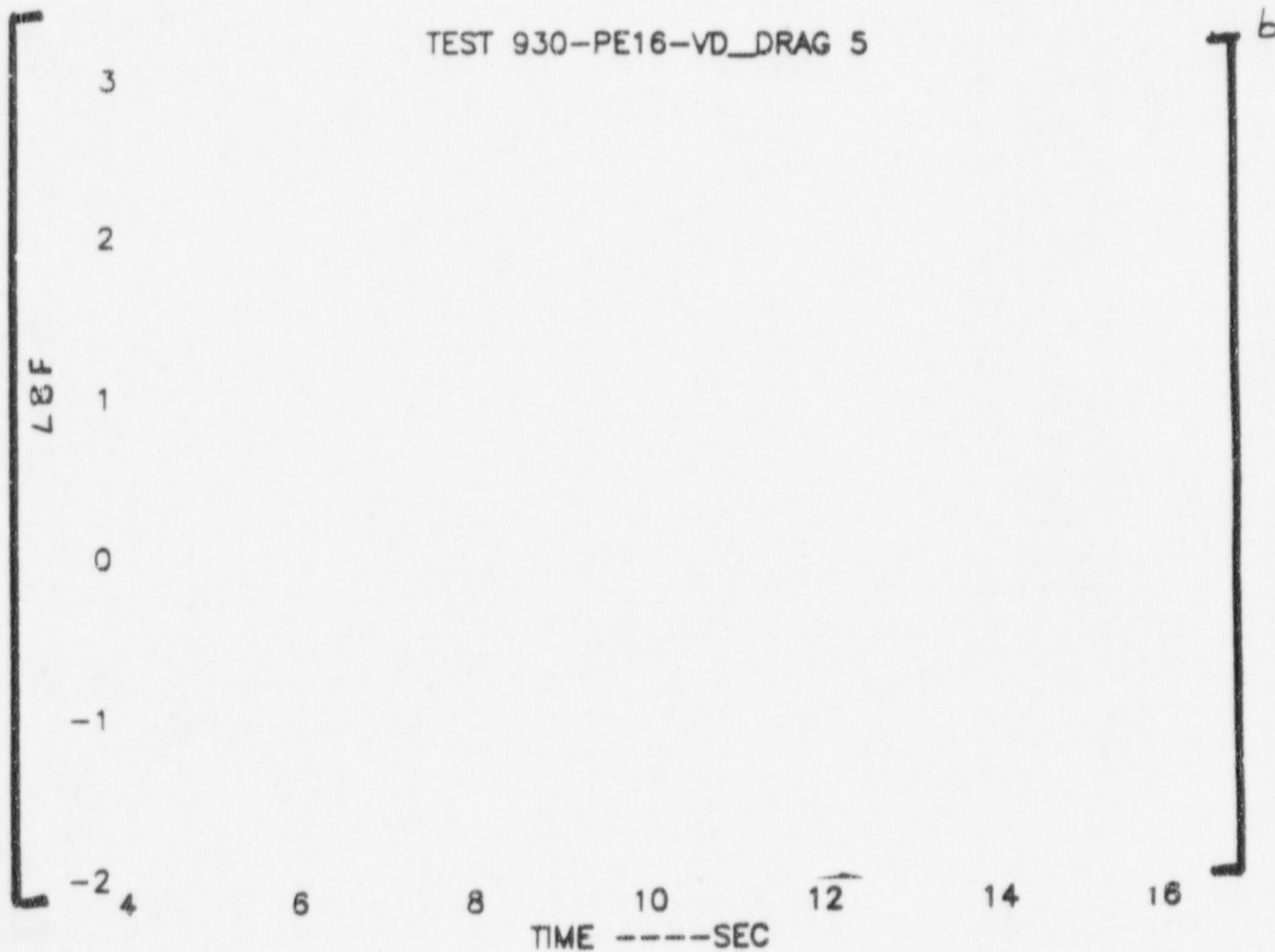


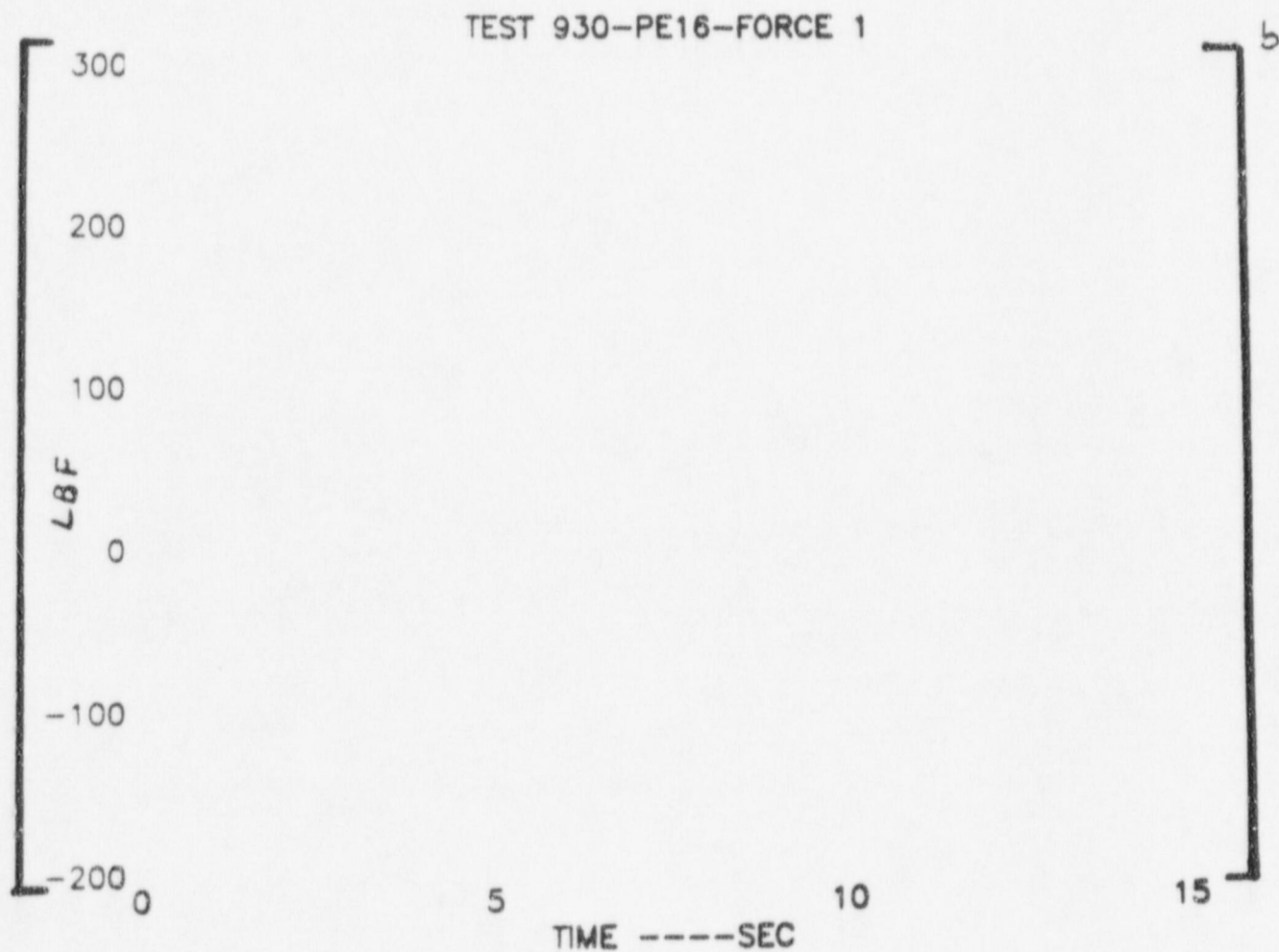
11. SOURCE STRENGTH TIME-HISTORYFT³/S

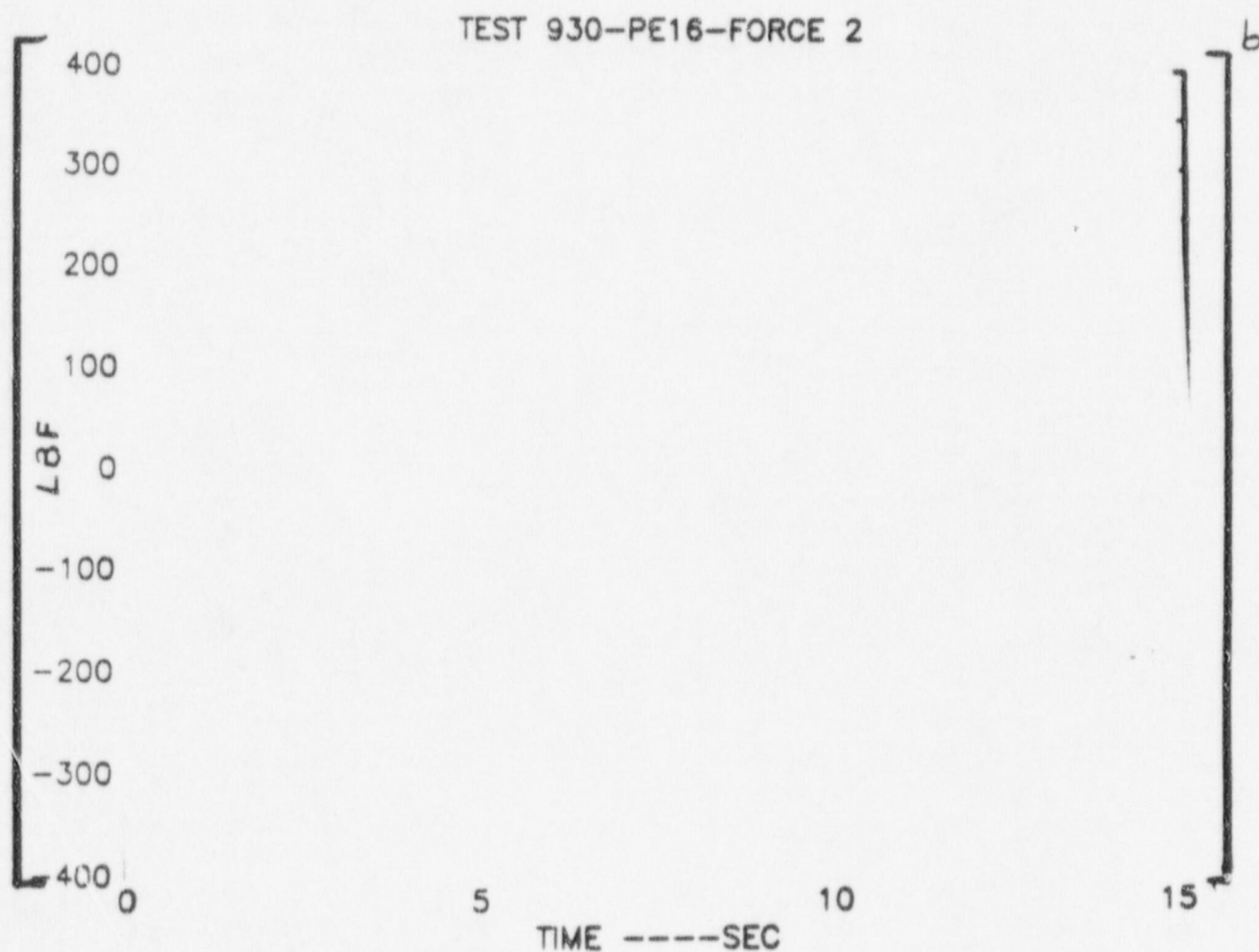
12. BUBBLE SURFACE VELOCITY TIME-HISTORY --- FT/S



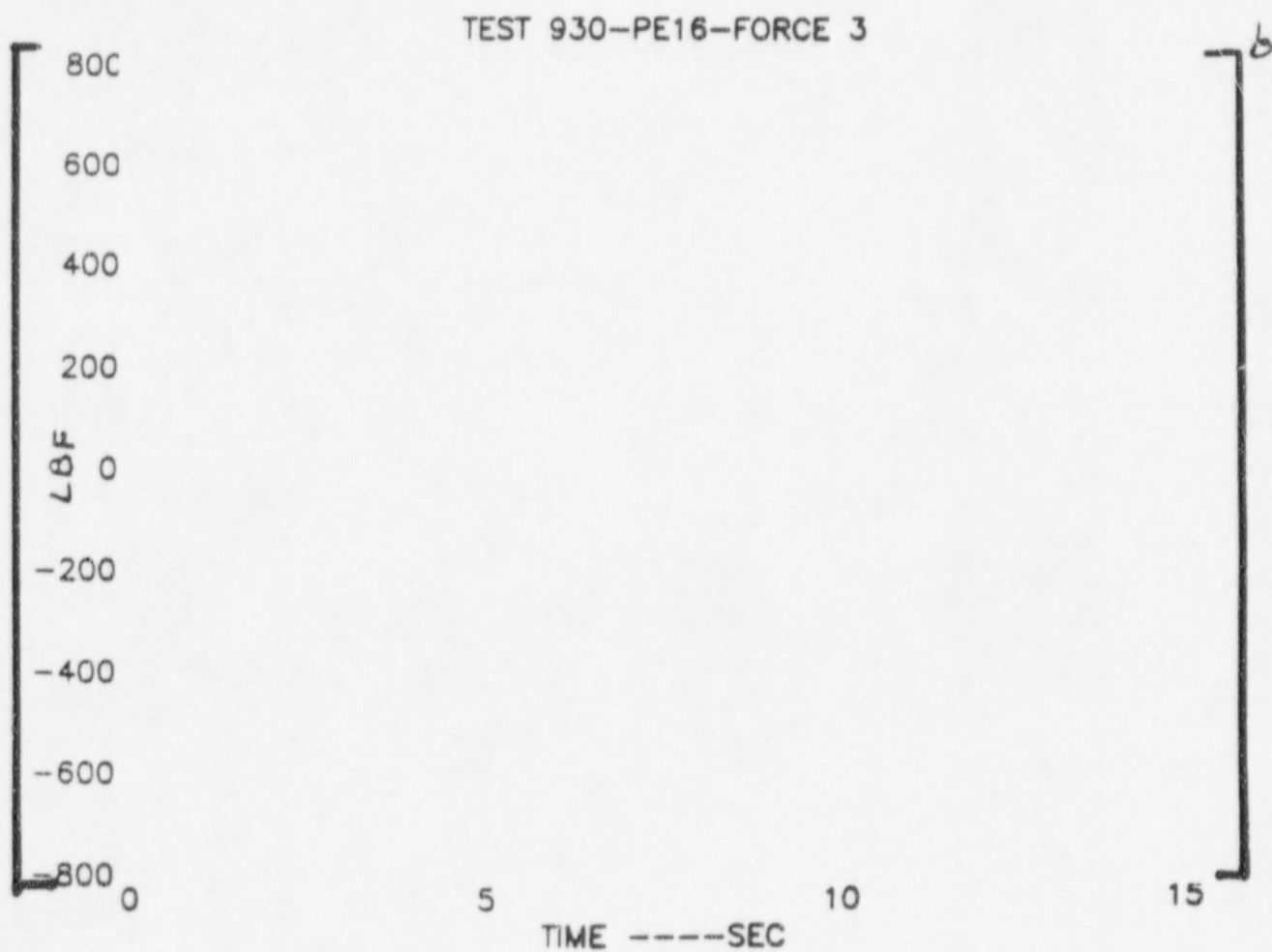
14. AD DRAG WITH REFERENCE TO 5TH ELEMENT (LBF)

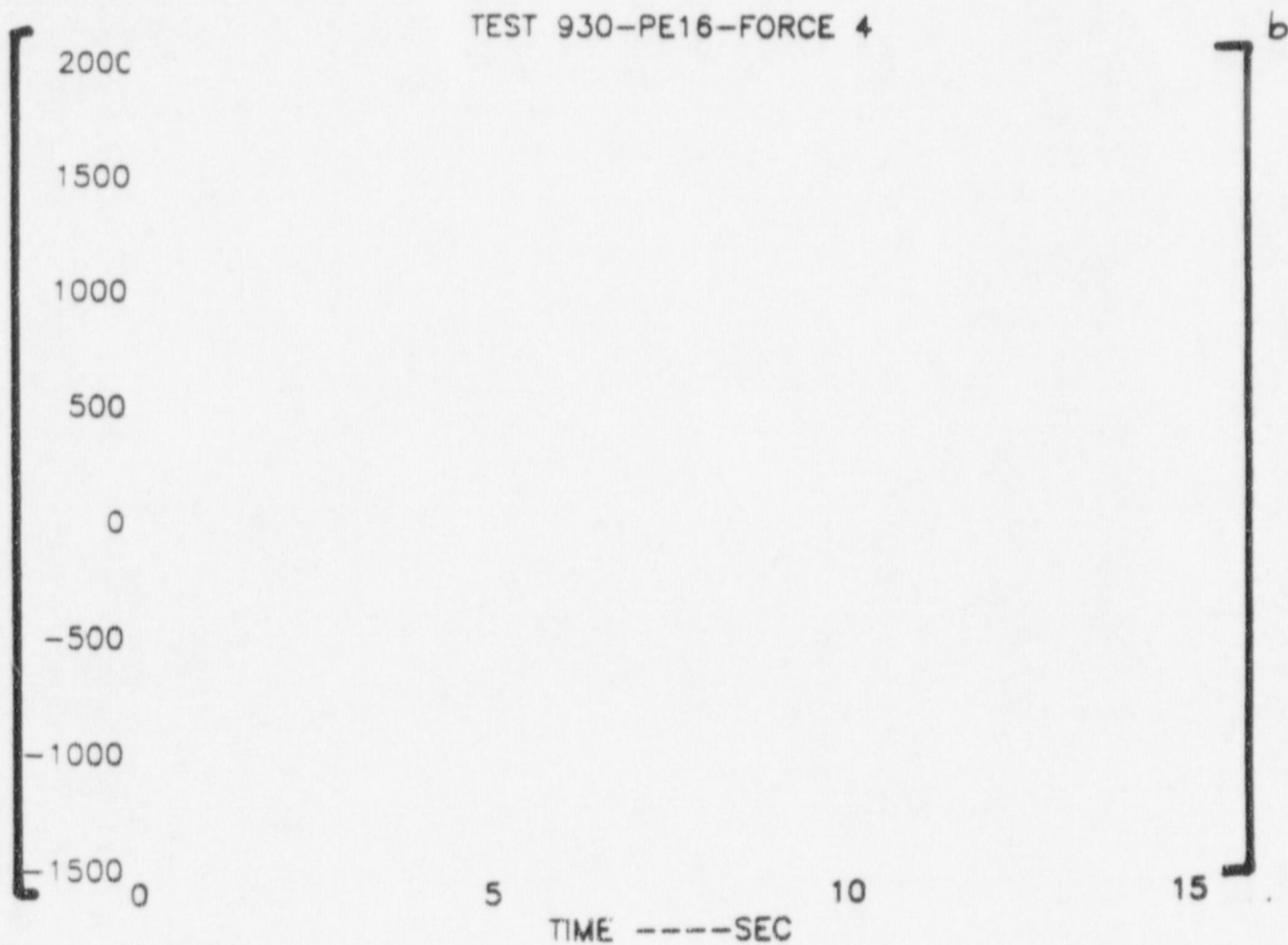
15. VD DRAG WITH REFERENCE TO 5TH ELEMENT (LBF

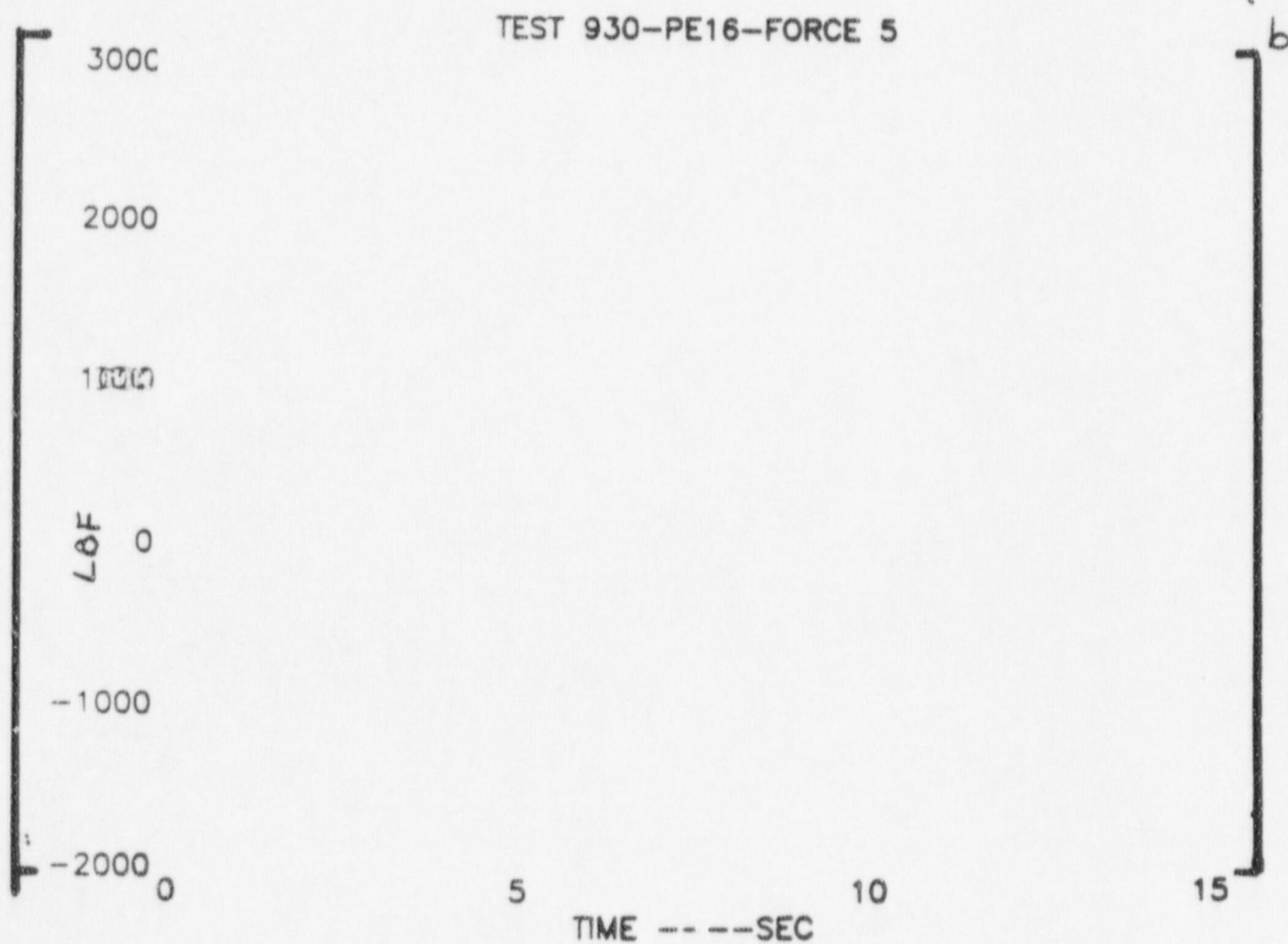
16. TOTAL DRAG ON 1ST ELEMENT (B1) -(LBF)

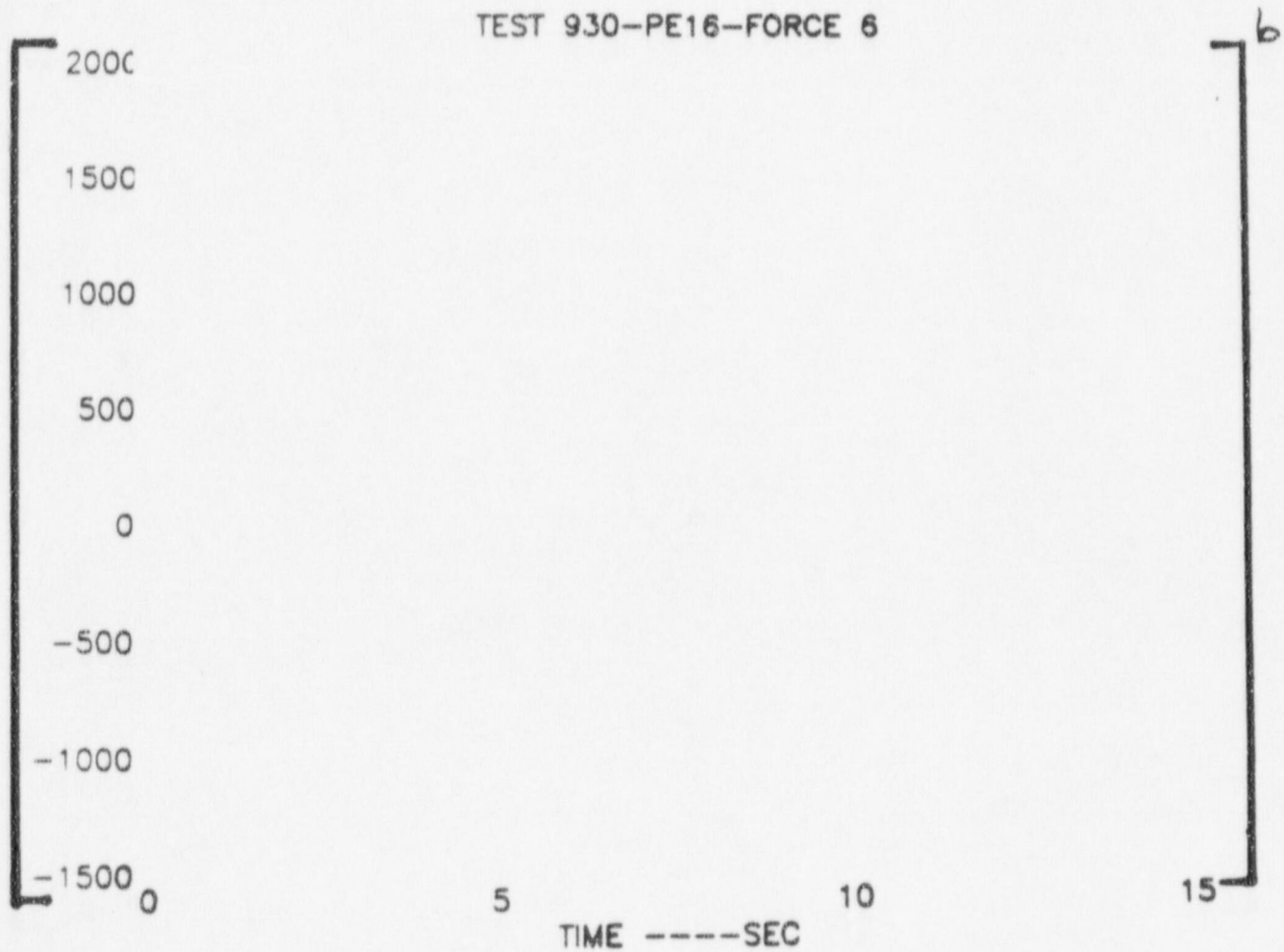
17. TOTAL DRAG ON 2ND ELEMENT (B2) -(LBF)

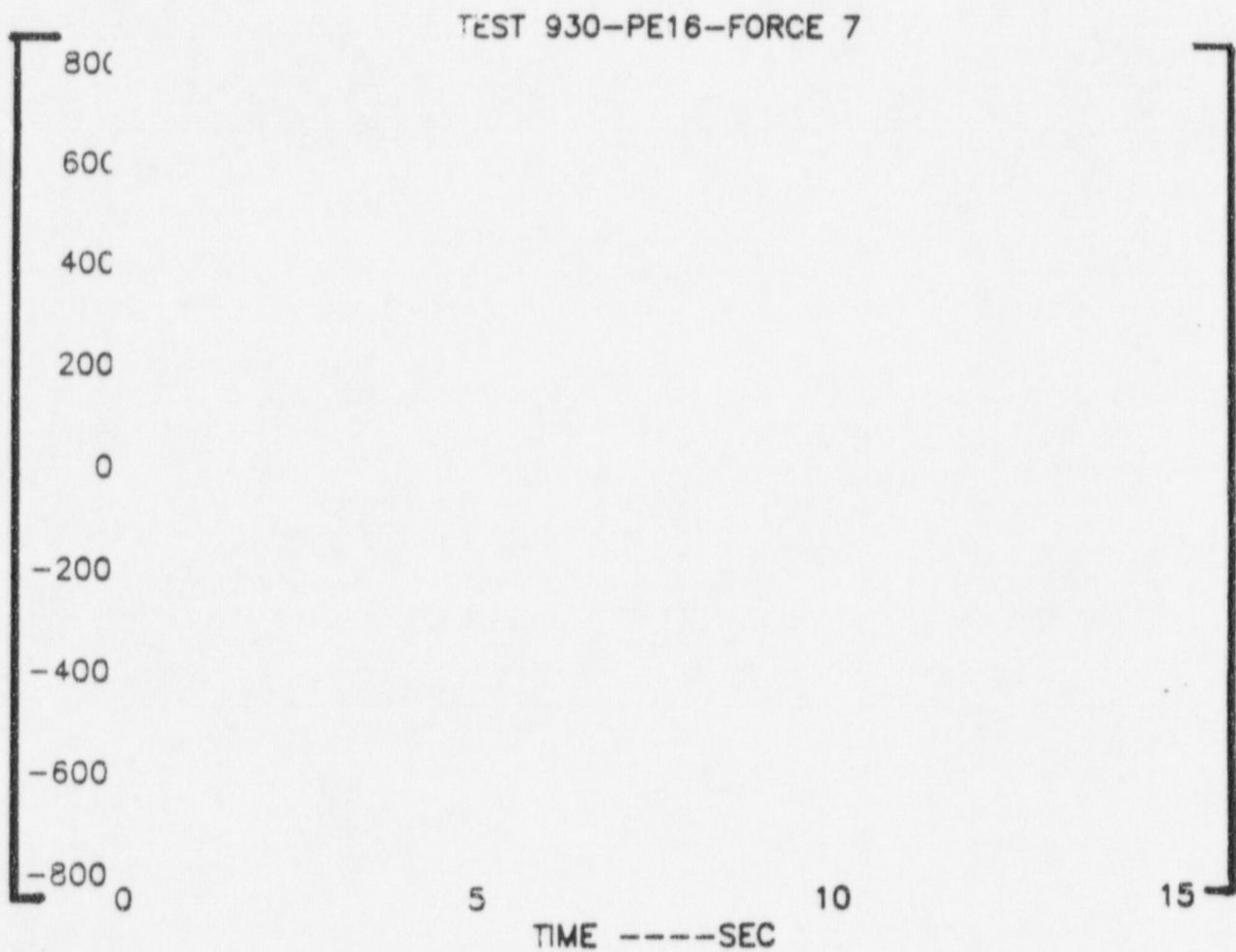
18. TOTAL DRAG ON 3RD ELEMENT (B3) -(LBF)

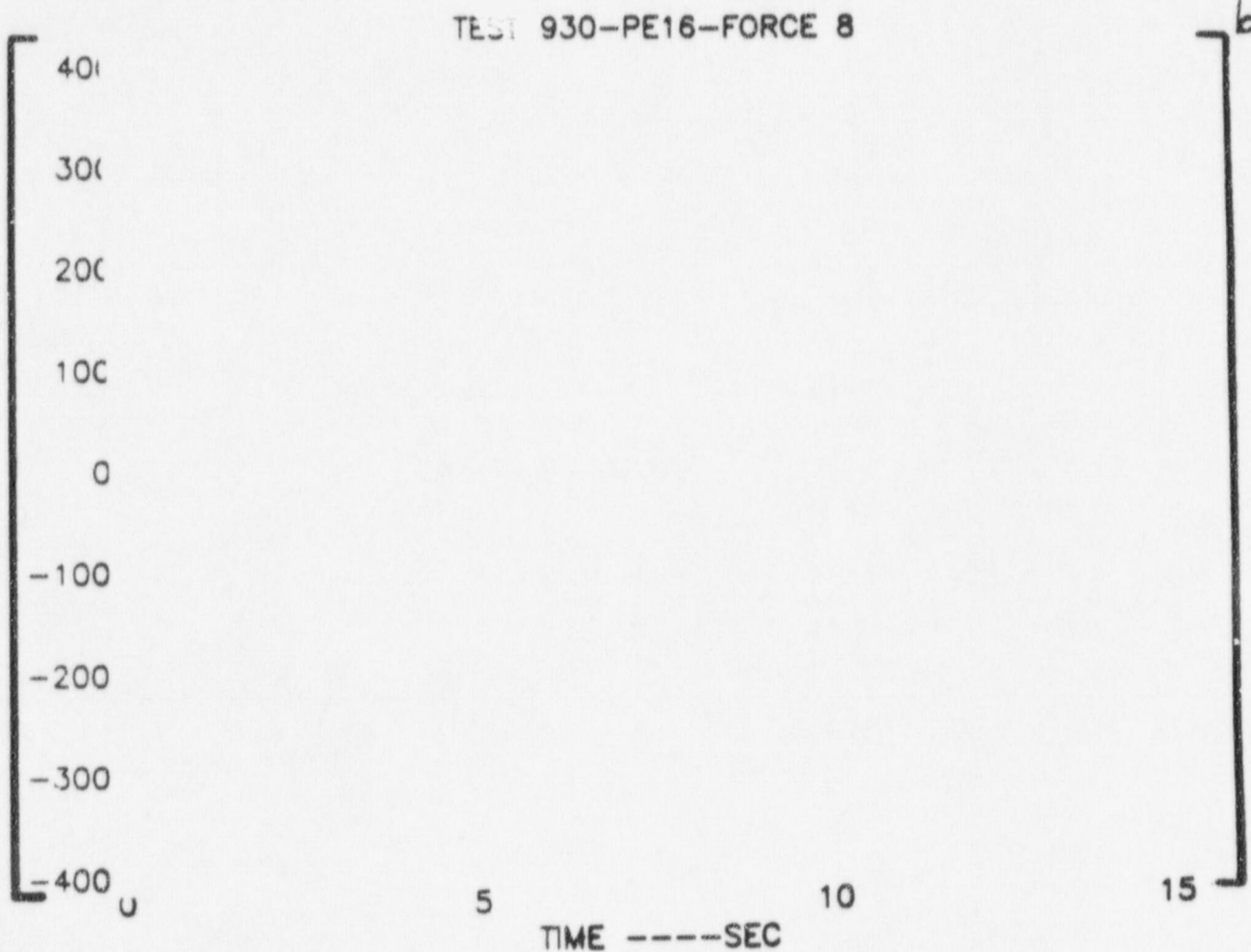


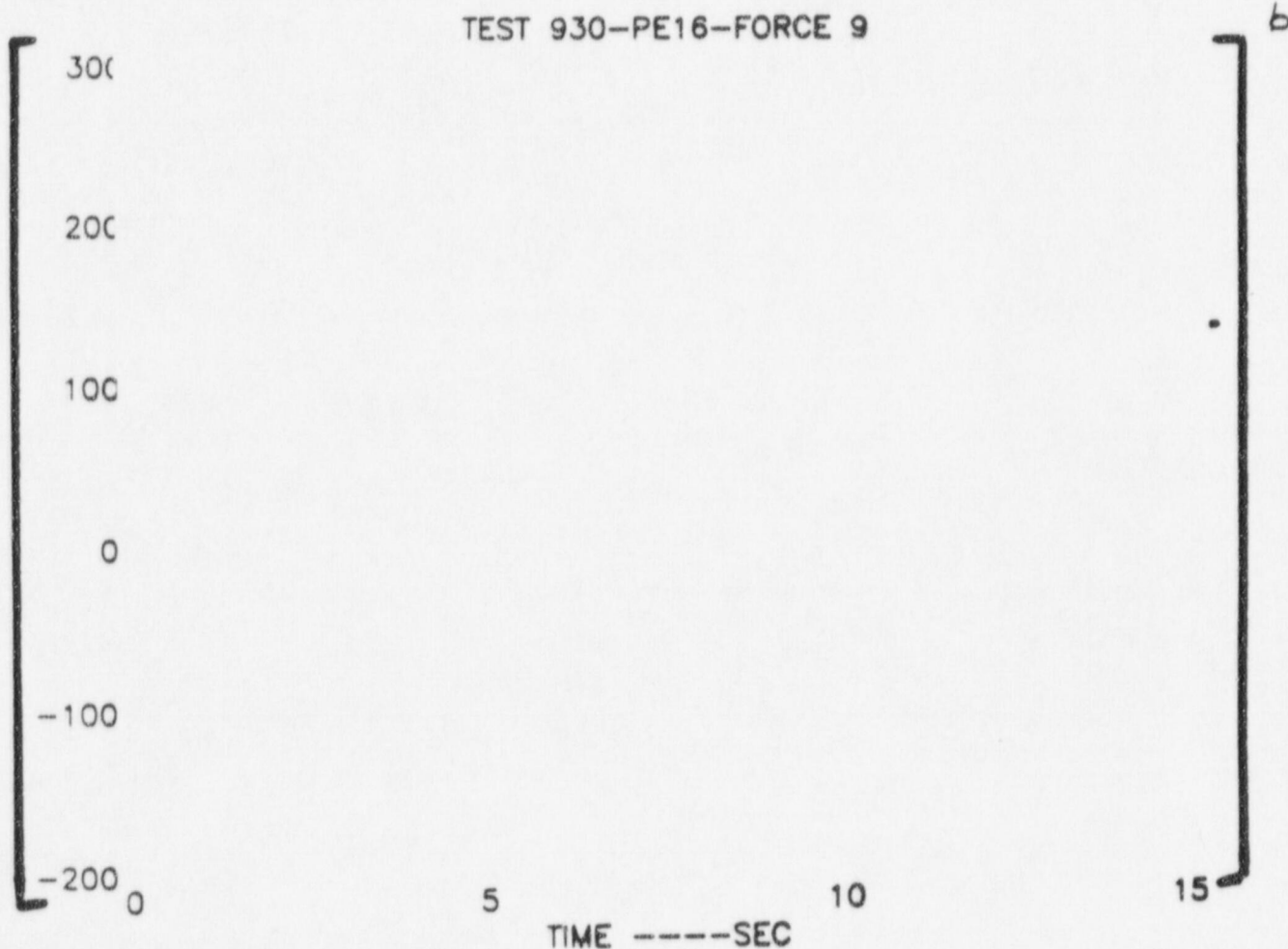
19. TOTAL DRAG ON 4TH ELEMENT (B4) -(LBF)

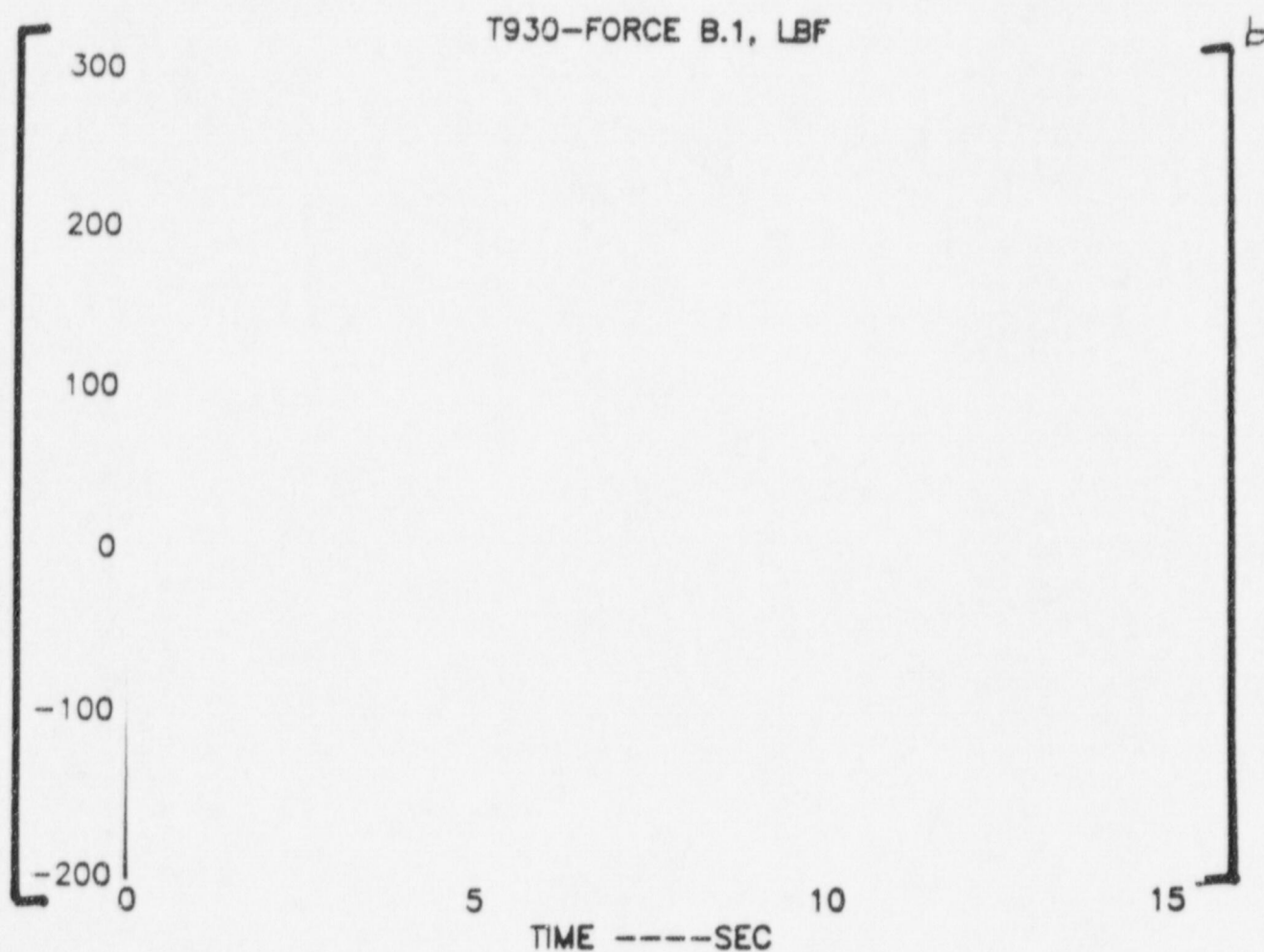
20. TOTAL DRAG ON 5TH ELEMENT (B5) -(LBF)

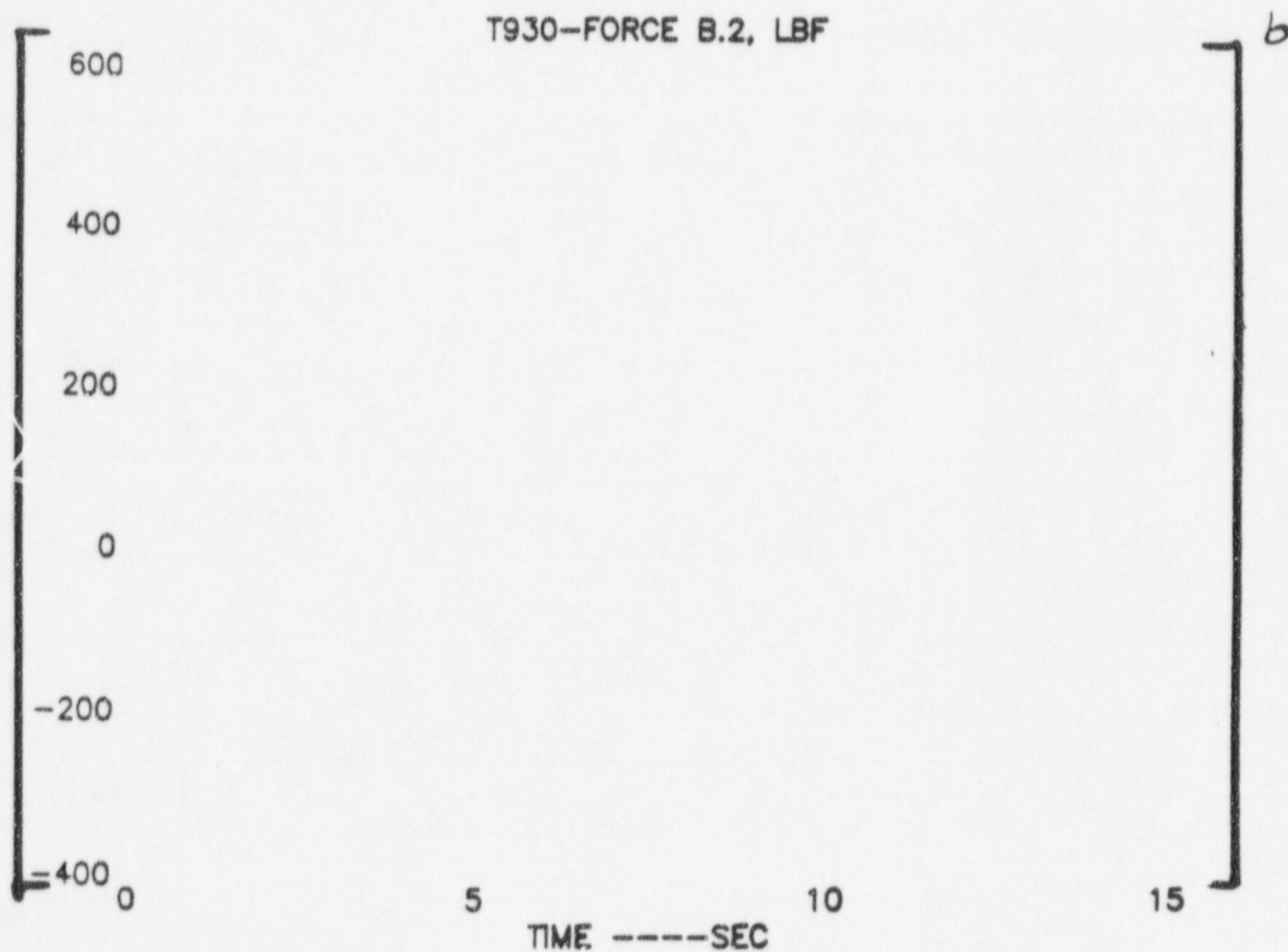
21. TOTAL DRAG ON 6TH ELEMENT (B6) -(LBF)

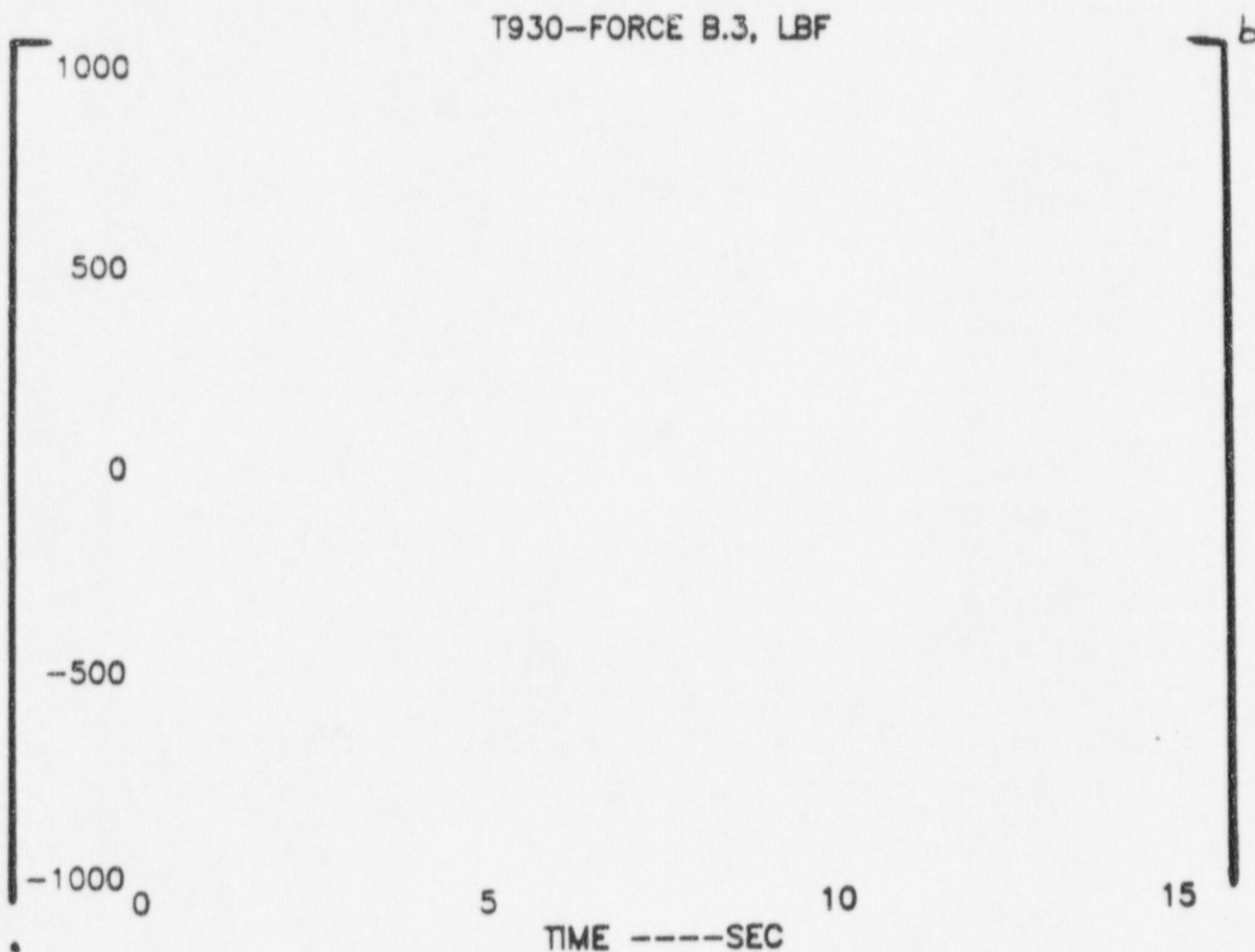
22. TOTAL DRAG ON 7TH ELEMENT (B7) -(LBF)

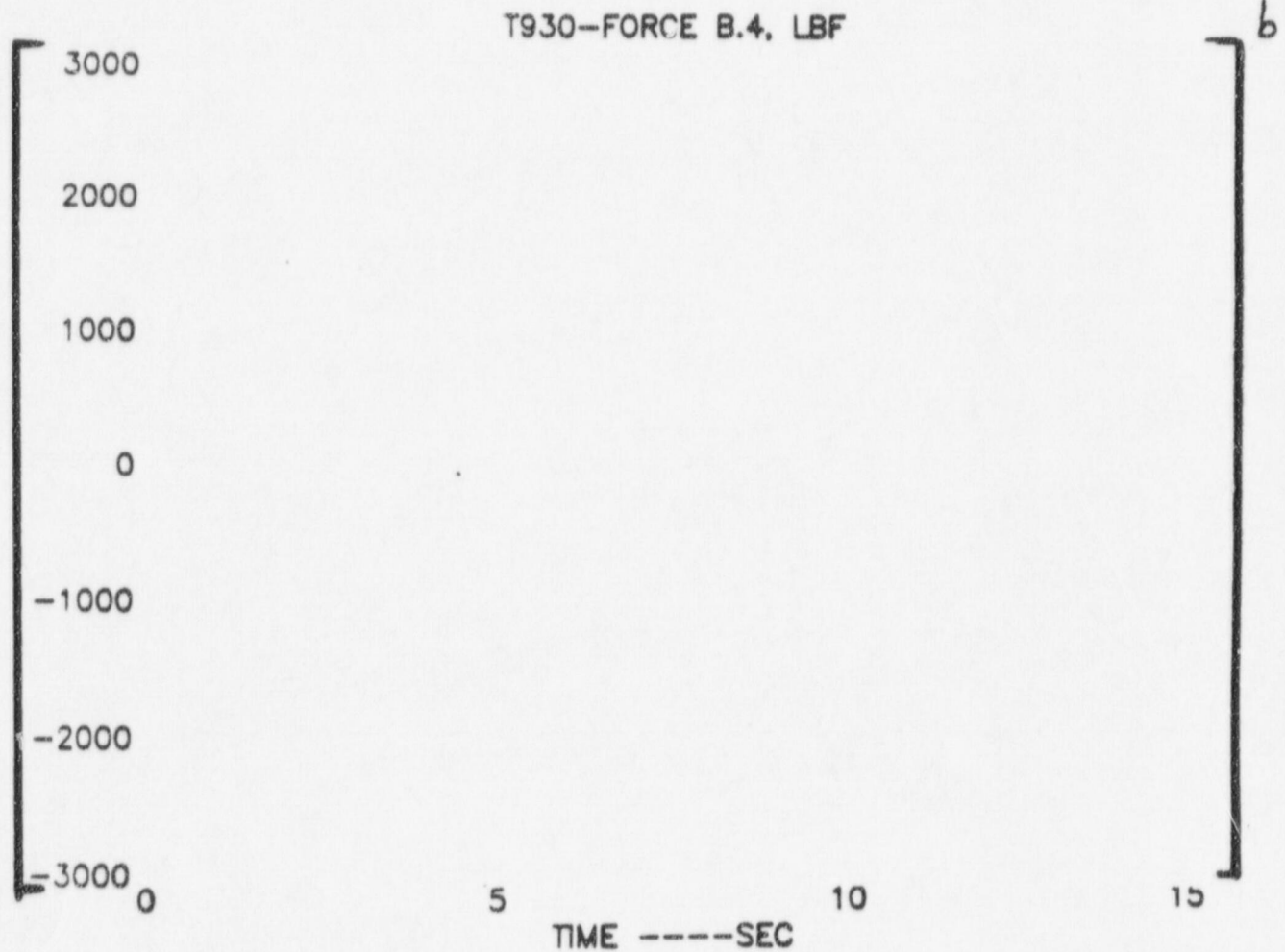
23. TOTAL DRAG ON 8TH ELEMENT (B8) -(LBF)

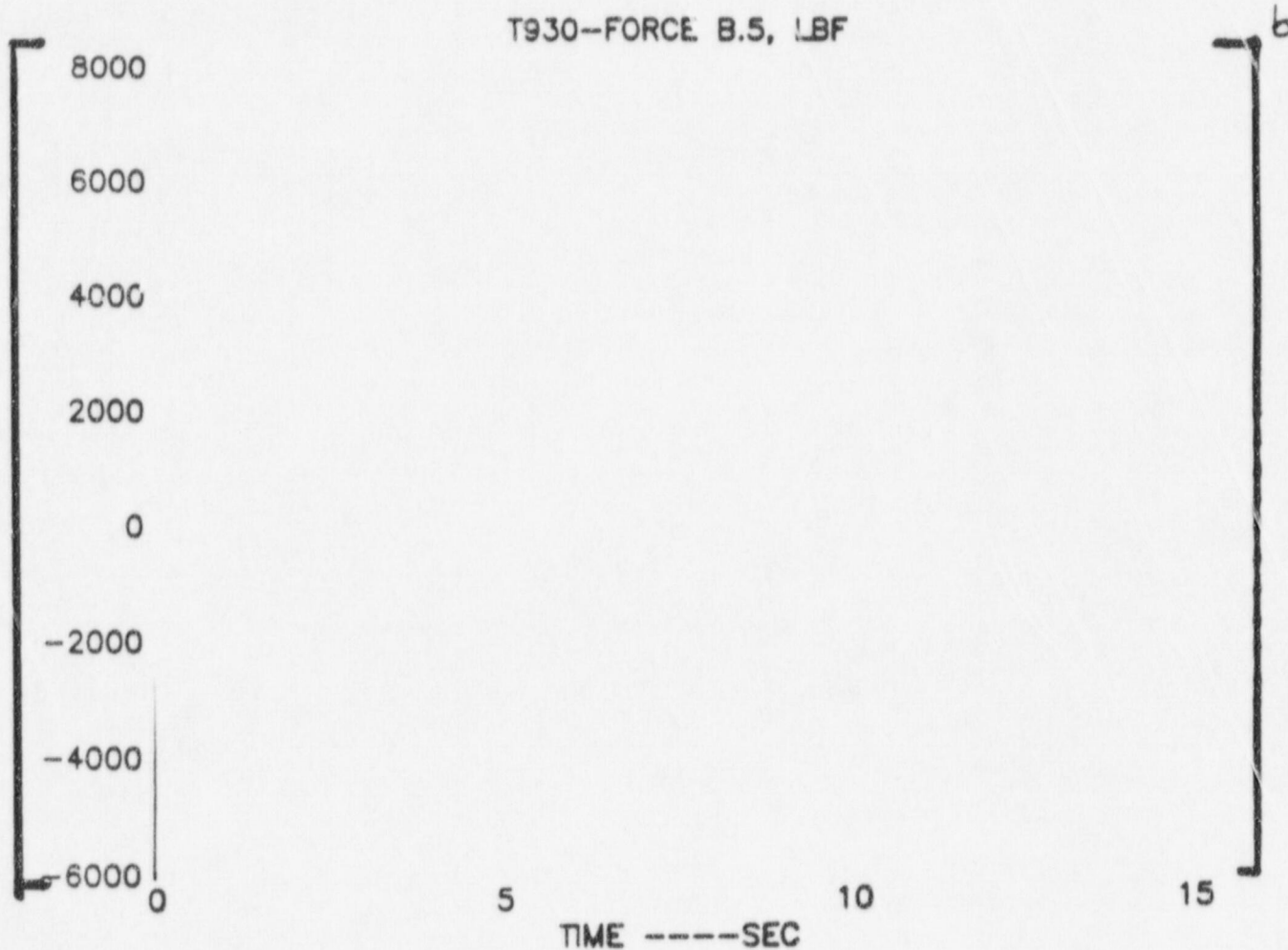
24. TOTAL DRAG ON 9TH ELEMENT (B9) -(LBF)

25. TOTAL DRAG ON 1ST ELEMENT (NODING: A---B) -(LBF)

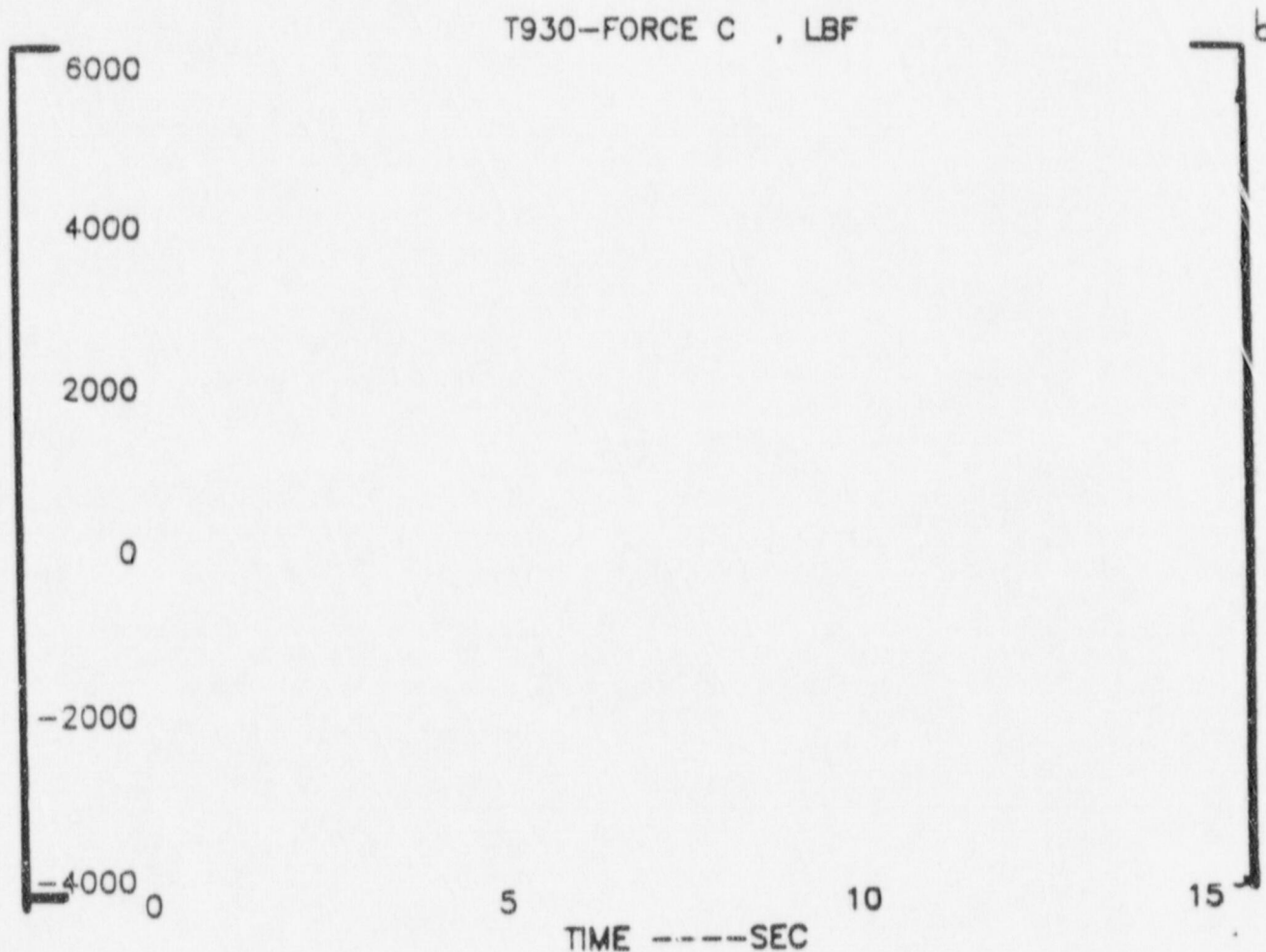
26. TOTAL DRAG ON 2ND ELEMENT (NODING: A---B) -(LBF)

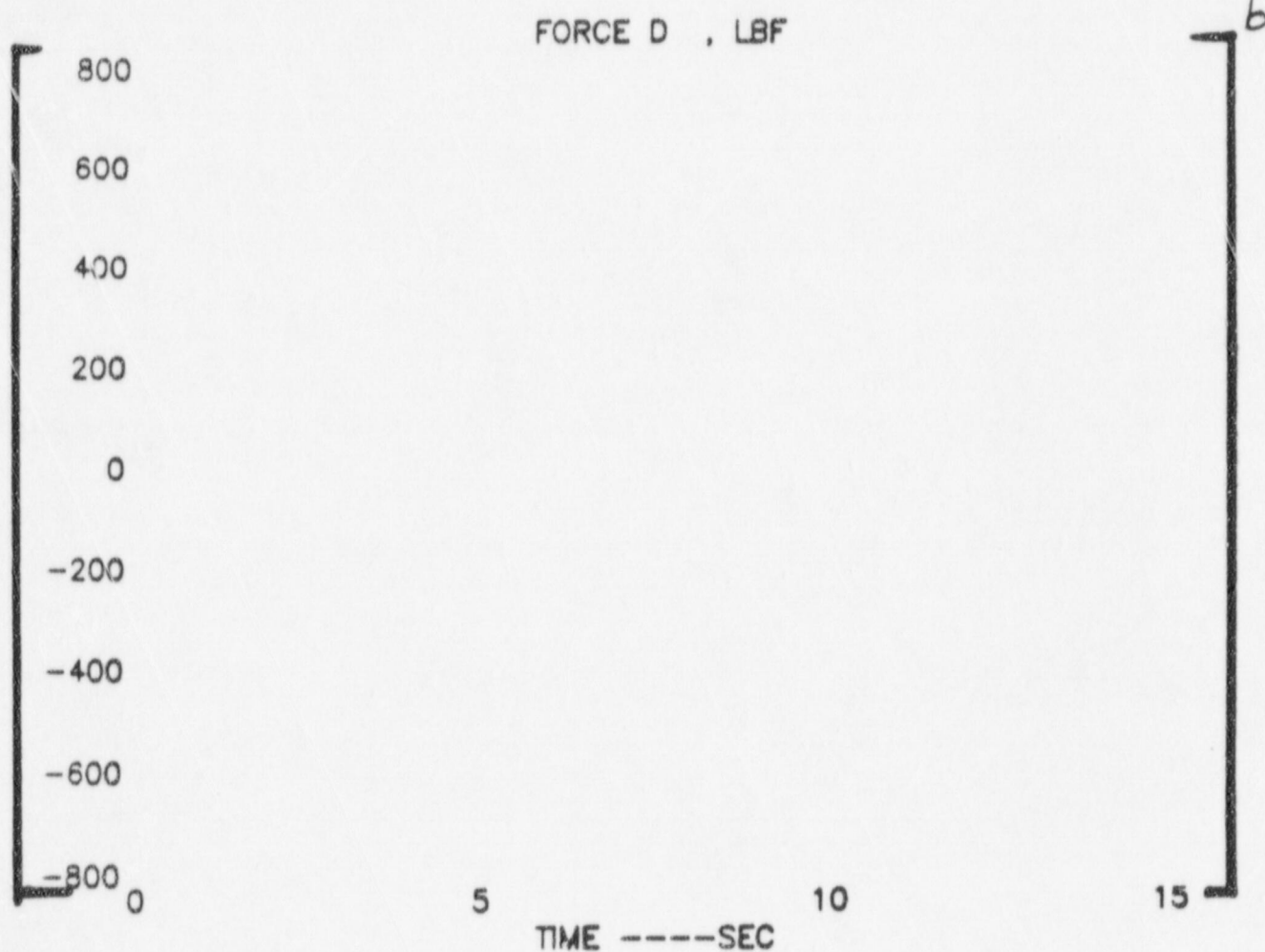
27. TOTAL DRAG ON 3RD ELEMENT (NODING: A---B) -(LBF)

28. TOTAL DRAG ON 4TH ELEMENT (NODING: A---B) -(LBF)

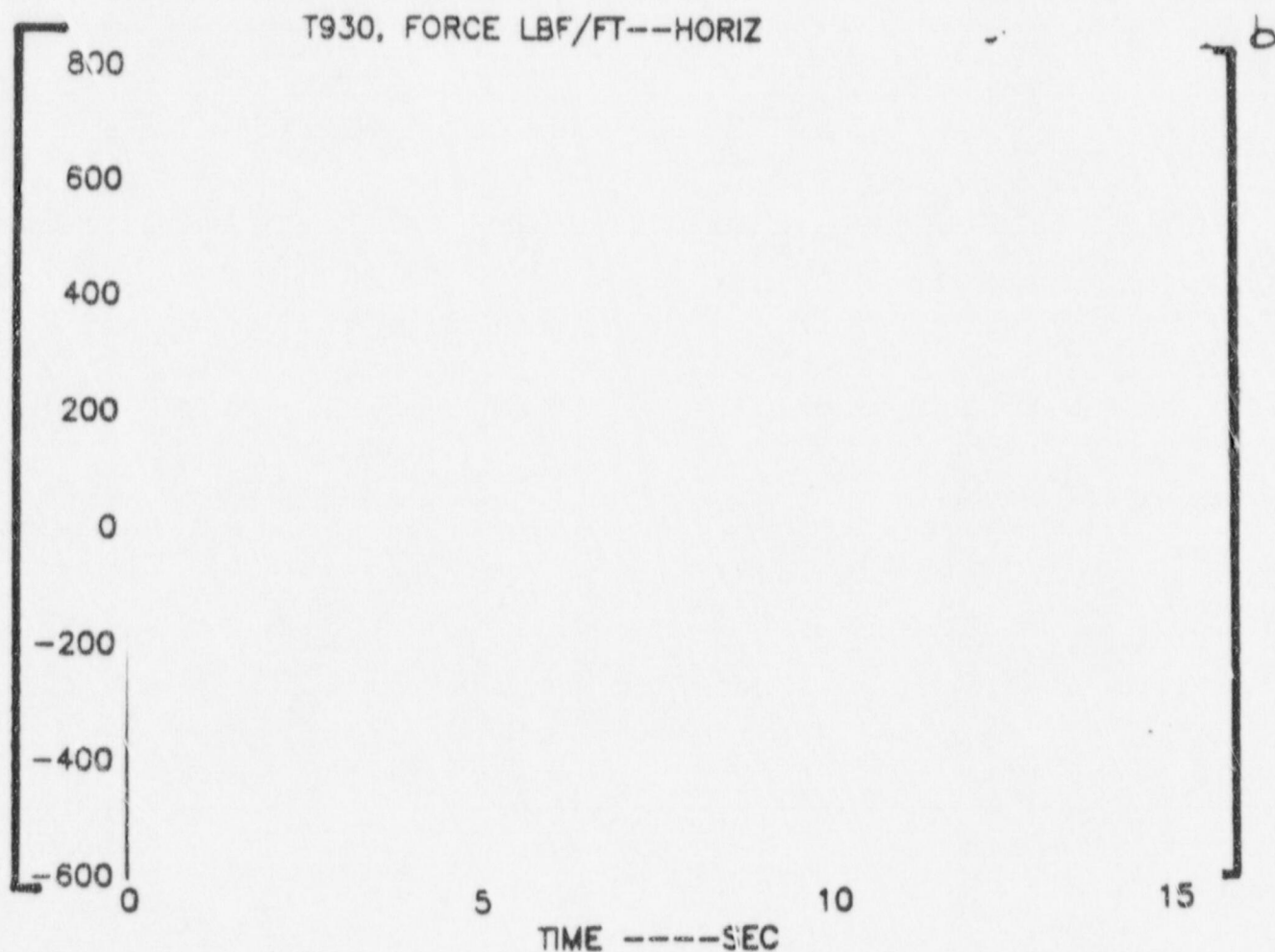
29. TOTAL DRAG ON 5TH ELEMENT (NODING: A---E) -(LBF)

30. TOTAL DRAG ON 6TH ELEMENT (NODING: B----C) (LBF)

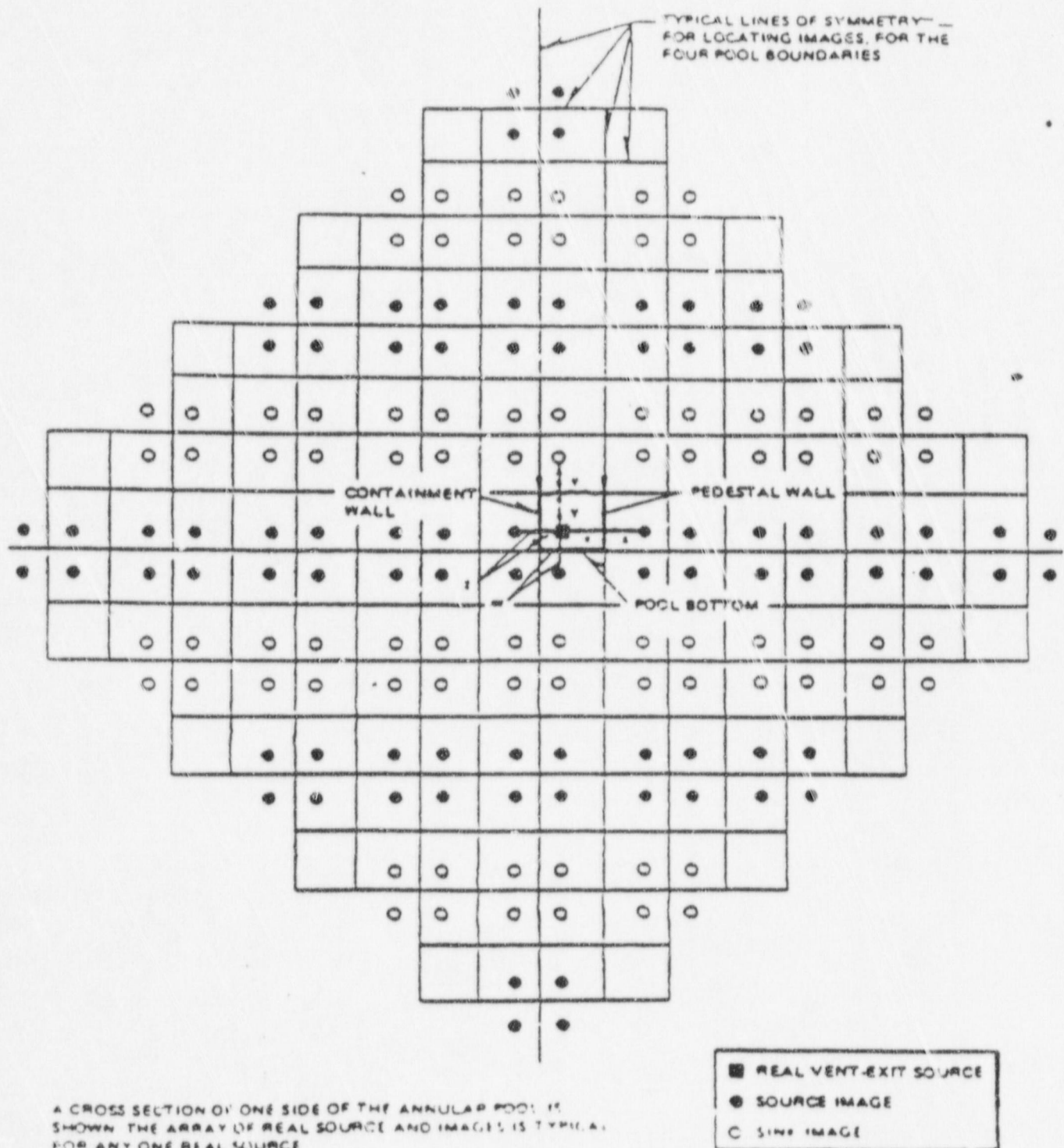


31. TOTAL DRAG ON 7TH ELEMENT (NODING: C---D---BEND) -(LBF)

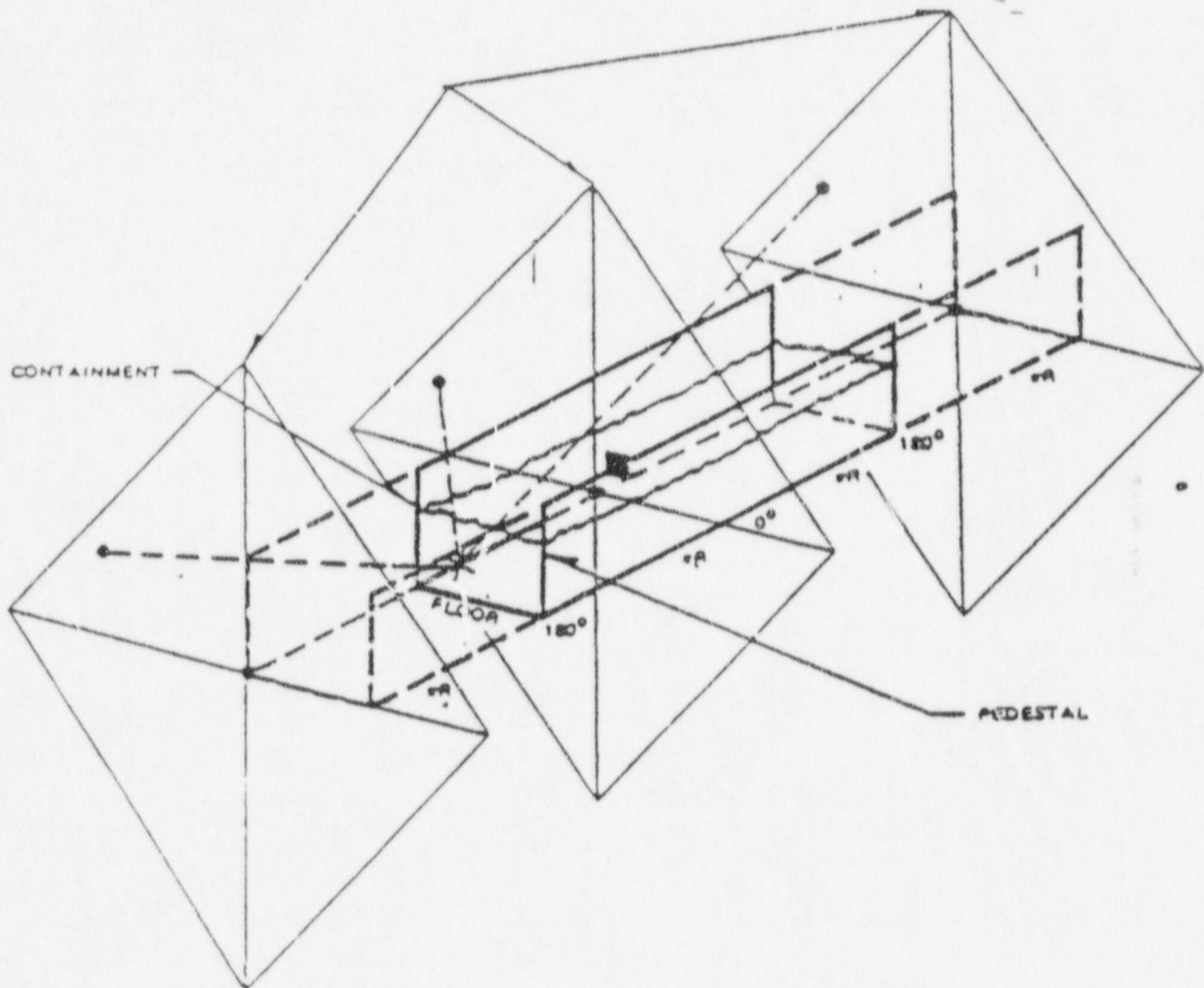
32. TOTAL DRAG ON A ONE-FOOT ELEMENT OF HORIZONTAL PIPING (lbf/ft)



33. PRECCI IMAGE PATTERN (8 DIAMONS)



34. PRECC1 3-DIMENSIONAL MODELING



- ACTUAL SOURCE AT VENT EXIT
- TYPICAL IMAGE SOURCE
- IMAGE-TO-NODE DISTANCES

35. UNIFORM FLOW PAST A STATIONARY STRUCTURE

